PEOPLE'S DEMOCRATIC REPUBLIC

OF ALGERIA

MINISTRY OF HIGHER EDUCATION

AND SCIENTIFIC RESEARCH

University of Kasdi Merbah Ouargla

Faculty of New Technologies of Information and Communication

Department of Electronics and Telecommunications

MASTER

Field: Science and Technology

Specialty: Telecommunications Systems

Theme:

Multimodal Biometric System Utilizing Palm Vein and Finger Vein Recognition

Prepared by:

- Khelil Raouia
- Khenfer Djahida

Submitted to the Jury Composed of:			
Samai Djamel	Professor	President	University of Ouargla
Chaa Morad	Professor	Supervisor	University of Ouargla
Korichi Maarouf	MCA	Co-Supervisor	University of Ouargla
Chebbera Fouad	Professor	Examiner	University of Ouargla

Academic Year: 2023/2024

إهداء

"الحمد لله على البدء و الختام الحمد لله على القوة والصبر الذي منحنا إياها طوال رحلتنا الدراسية شكرنا يتوجه في المقام الأول إلى الله عزوجل الذي أنار طريقنا بنور المعرفة والعلم، ولإرادته في إتمام هذا العمل".

"إلى كل من ساهم بشكل مباشر أو غير مباشر في إتمام هذه المذكرة، أرغب في تقديم فائق الشكر والامتنان. إنه لشرف كبير أن أكون جزءًا من هذا المجتمع الأكاديمي المتميز، وأن أتشارك معكم هذا الإنجاز الذي لن ينسى".

"إلى من كلل العرق جبينه.. إلى من علمني العطاء بدون انتظار .. إلى من أحمل أسمه بكل افتخار .. رحمك الله و تقبلك من الشهداء , ستبقى كلماتك نجوم أهتدي بها اليوم و غدا وإلى الأبد .. والدي العزيز **مفتاح خنفر** رحمه الله" .

"إلى من كانت الداعم الأول لتحقيق طموحي .. إلى من كانت ملجأي ويدي اليمنى في دراستي إلى من أبصرت بها طريق حياتي و اعتزازي بذاتي .. إلى القلب الحنون إلى من كانت دعواتها تحيطني .. والدتي العزيزة **مسعودة خنفر**" .

"إلى ضلعي الثابت و أمان أيامي إلى من شددت عضدي بهم فكانوا ينابيع أرتوي منها.. إلى إخواني الغاليين "

" لكل من كان عونا وسندا في هذا الطريق .. للأصدقاء الأوفياء ورفقاء السنين لأصحاب الشدائد و الأزمات .. إلى حصيلة سنواتي صديقاتي .. ميار .. سيرين .. وئام .. كوثر .. إكرام ".

"إلي من حصد الأشواك عن دربي .... إلي قدوتي... و السراج الذي لا ينطفي نوره أبدا .....إلي من كان سندي و قوتي إلي من علمني أن للسماء حدود .....إلي من بذل جهد السنين لاعتلي سلالم النجاح .....والدي العزيز دمت لي ذخرا **" خليل عمر"**

"إلي من اخص الله الجنة تحت قدميها..... رمز الحب و بلسم الشفاء ..... إلي القلب الناصع بالبياض .... و التي يتجاوز وصفها الثمانية و العشرون حرف..... داعمتي الأولي في كل خطوة..... إلي من علمني الصبر و العمل الجاد أمي قرة عيني حفضها الله **" شاهد مريم "**

"إلي من كانوا جناحي الأيمن ... و سند الحياة .....مصدر راحتي إخواني الأعزاء .... إلي من كان دائما مصدر للفرح و السعادة أخي الصغير **"انس "**

"إلي من كانوا دعماً وسنداً في أوقات الصعاب في هذه المسيرة رفقاء دربي الأوفياء..مهدية... مني .. مارية.... جهان ."

"إلي من كانت دعواتهم تلازمني دائما ... عائلتي دمتم لي شيئا لا ينتهي".

"إلى كل هؤلاء أهديهم هذا العمل المتواضع, سائلا الله العلي القدير أن ينفعنا به ويمدنا بتوفيقه ."

Acknowledgment

Almost at the end of my university journey, after five years of perseverance and toil in pursuit of knowledge, carrying within it the aspirations of countless nights. Today, I stand at the threshold of graduation, reaping the fruits of my labor, lifting my cap with pride. Thank you, O God, for your praise even before my satisfaction, for your praise upon satisfaction, and for your praise after satisfaction, as you enabled me to achieve this success and fulfill my dream.

I want to express my deep gratitude to my professors and thesis supervisor, Professor **"Chaa Mourad",** who was always attentive and available to us throughout the process of completing this thesis. Thank you very much for your accessibility, for the numerous stimulating academic discussions, for the constructive feedback and guidance, for the many wise pieces of advice, for the continuous support, for your understanding, for the trust you bestowed upon us, and for your time throughout this academic journey. You have been a source of inspiration and an example of dedication and diligence, and I will not forget the value of your contributions to my success.

Also, I cannot overlook Engineer **"Djamel Medjoudj"** for his assistance throughout the period of completing this thesis, as well as my dear colleagues**"Nacer eddine Dellah"**who shared every moment with me on this journey. You have been a constant source of support and motivation for me, and I will not forget any of the beautiful memories we shared together.

I hope this thesis serves as a modest contribution to the field I have chosen and adds value to society. I look forward eagerly to a bright future filled with challenges and opportunities.

ملخص : تزداد شعبية المصادقة البيومترية نظرًا لأمانها العالي وسهولة استخدامها مقارنة بالطرق التقليدية تعتمد هذه التقنيات على الصفات الفريدة لكل فرد، مثل الأوردة تحت الجلد.حيث تقدم التقنية مقاومة اكبر للتزوير(صعوبة الوصول للأوردة تحت الجلد) والظروف البيئية، وتستخدم في مجالات متنوعة حيث أن الأوردة تحت الجلد لا تظهر إلا في ضوء الأشعة تحت الحمراء القريبة. الهدف من عملنا هو زيادة دقة التعرف على الأفراد عن طريق اوردة كف اليد اليمنى اليسرى و اوردة اصبع السبابة الايسر باستخدام تقنيات استخراج الميزات حيث نبدأ باستخراج منطقة الاهتمام (ROI) حيث يتمثل ذلك في اختيار أفضل جزء من الصورة لاستخراج الميزات اللاحقة يتمثل اقتراحنا في استخدام تقنيات استخراج الميزات باستخدام مرشحي GABOR و LPQ. وفي النهاية، يتم تصنيف الميزات باستخدام خوارزميات KNN بمسافات مختلفة الأبعاد (الأبعاد الاقليدية، الكوسين، CTB، ماهكوس). حيث أظهرت دراستنا أداءً مشجعًا للغاية، حيث بلغ معدل التعرف على الأفراد 100%.

كلمات مفتاحيه : المصادقة البيومترية ,الأوردة , ضوء الأشعة تحت الحمراء القريبة ,منطقة الاهتمام , تكميم المرحلة المحلية , فلتر غابور, KNN .

Abstract:

Biometric authentication is gaining popularity due to its high security and ease of use compared to traditional methods. These technologies rely on unique individual traits, such as subcutaneous veins. The technology offers greater resistance to forgery (due to the difficulty of accessing subcutaneous veins) and environmental conditions, and is used in various fields where subcutaneous veins are only visible under near-infrared light. Our goal is to increase individual recognition accuracy using the veins of both right and left palms and the left index finger, employing feature extraction techniques. This involves starting with the extraction of the Region of Interest (ROI), selecting the best part of the image for subsequent feature extraction. Our proposal includes using feature extraction techniques with GABOR and LPQ filters. Finally, features are classified using KNN algorithms with various distance metrics (Euclidean, Cosine, City Block, Mahalanobis). Our study demonstrated highly encouraging performance, achieving a recognition rate of 100%.

Key words: Biometric authentication, Veins, Near-infrared light, ROI, LPQ, GABOR filter bank, KNN.

Résumé :

La popularité de l'authentification biométrique augmente en raison de sa haute sécurité et de sa facilité d'utilisation par rapport aux méthodes traditionnelles. Ces technologies reposent sur des traits individuels uniques, tels que les veines sous-cutanées. La technologie offre une plus grande résistance à la contrefaçon (en raison de la difficulté d'accès aux veines sous-cutanées) et aux conditions environnementales, et elle est utilisée dans divers domaines où les veines sous-cutanées ne sont visibles qu'à la lumière infrarouge proche. Notre objectif est d'augmenter la précision de la reconnaissance individuelle en utilisant les veines des paumes droite et gauche ainsi que l'index gauche, en utilisant des techniques d'extraction de caractéristiques. Cela implique de commencer par l'extraction de la Région d'Intérêt (ROI), en sélectionnant la meilleure partie de l'image pour l'extraction ultérieure des caractéristiques. Notre proposition inclut l'utilisation de techniques d'extraction de caractéristiques avec les filtres GABOR et LPQ. Enfin, les caractéristiques sont classées à l'aide d'algorithmes KNN avec diverses distances (Euclidienne, Cosinus, Bloc de Ville, Mahalanobis). Notre étude a montré des performances très encourageantes, atteignant un taux de reconnaissance de 100%.

Mots-clés : Authentification Biométrique, Veines, Lumière proche infrarouge, ROI, LPQ, Banc de filtres de Gabor, KNN.

Table of Content

Chapter II: The state of the art of hand vein

Chapter III: Result and discussion

List of figures

List of tables

Acronyms:

CMC: (Cumulative Match Characteristic)

DET: (Detection Error Tradeoff)

EER: (Equal Error Rate)

FAR: (False Acceptance Rate)

FKP: (Finger knuckle print)

FRR: (False Reject Rate)

KNN: (k-Nearest Neighbors)

LPQ: (Local Phase Quantization)

NIR: (near-infrared)

ROC: (Receiver Operating Characteristic)

ROI: (Region of Interest)

SVM: (Support Vector Machine)

Introduction general

Information systems security has become an area of great research interest. Identification of individuals is a pivotal element of the security framework, necessary to ensure the security of systems and institutions. Individual recognition has gradually gained importance in daily human activities, facilitating secure transactions across various sectors. Although originally limited to fields such as the military and medicine, recognition systems are now widely applied, including controlling access to devices and facilities, as well as protecting financial assets such as bank cards

The term "biometrics" is increasingly common in our daily lives, with its origins tracing back to the 19th century. Various biometric technologies have since been developed, relying on physiological and behavioral identifiers like the iris [1], voice [2], fingerprints [3], face [4], signature, etc. These technologies are deemed more reliable than traditional systems such as keys or passwords due to their resistance to forgery. They enable precise and unique recognition of individuals based on their distinct biometric characteristics. This has spurred a rising demand for biometric systems, with advancements now encompassing vein recognition (palm and finger).

The technology of vein recognition, also known as vascular biometrics, involves capturing and analyzing unique vein patterns in the body for biometric identification. This process uses optical scanning to capture vein images in areas like the palm and fingers, making it highly secure due to the sub-dermal nature of veins. This method leverages the distinctiveness and stability of vein patterns, which are unique to each individual and remain constant over time [5].

In the case of hand vein recognition, whether in civilian or public contexts, it essentially involves comparing two images of complete prints with controlled quality. In this study, we chose a recognition system based on both hand veins and finger veins. This system uses the shape of the inside of the hand and fingers to extract biometric characteristics that allow individuals to be identified. These characteristics are permanent and stable throughout life and are unique to each individual, even for identical twins [6].

Features are extracted using techniques such as LPQ (Local Phase Quantization) method and Gabor filter bank. These methods enable the extraction of specific and discriminative information from palm vein and finger.

For classification, the KNN (k-nearest neighbors) algorithm is employed. It categorizes palm and finger vein vectors based on their similarity. Various metrics are utilized to measure similarity, including Euclidean distance, cosine similarity, city block distance, and Mahalanobis distance.

Our work is divided into three distinct chapters:

Chapter 01: In this chapter, we elucidate the concept of biometrics, along with its characteristics and modalities, encompassing both physiological and behavioral aspects. Additionally, we explore the evaluations of biometric systems, offering insights into various methodologies employed to assess their performance and reliability.

Chapter 02: we explored the most recent techniques for extracting features from finger and palm vein. We delved into different methodologies and technologies utilized to derive unique and distinguishing features from hand vein prints. This enabled us to grasp the current methodologies and recent developments in this area**.**

Chapter 03: In this chapter, we comprehensively elucidated the methodology employed for representing hand vein patterns. We delineated each step of our approach, which encompasses feature extraction utilizing specific techniques such as LPQ and Gabor filters, vector classification utilizing the KNN algorithm with Mahcos distance, and the score-level fusion technique between palm vein and finger vein.

In this system, utilizing the aforementioned methods, we achieved perfect accuracy when applied to a database containing 42 individuals and 1050 images. The results were exceptional, achieving a Rank-1 recognition rate of 100%, an Equal Error Rate (EER) of 0.00%, and verification rates (VR) of 100% at false accept rate 1% and 0.1%.

In future work, we aim to expand the dataset by recruiting more participants and broadening it for verification purposes. Additionally, we plan to enhance image acquisition by developing high-quality imaging devices suitable for finger and palm veins.

Introduction:

In today's rapidly advancing technological landscape and growing dependence on digital information, the demand for efficient methods of identification and authentication has reached unprecedented levels. In this scenario, the emergence of biometric identification systems stands out as a critical tool across different domains. Throughout this chapter, we explored diverse and enduring biometric traits like fingerprints, facial features, or iris scans, which serve to authenticate and verify individuals' identities, offering higher accuracy and security compared to traditional methods reliant on passwords or smart cards .Biometric identification technologies offer a unique advantage, as an individual's biometric data cannot be easily copied or forged, making them more reliable in dealing with security systems and computers.

In this introduction, we will delve into the world of biometric identification systems in more detail, including their architecture, evaluation, as well as their applications in fields such as security, surveillance, and digital identity management.

I.1Biometrics definition:

Biometrics is a technology used for identifying and verifying individuals, involving the conversion of biological, morphological, or behavioral traits into digital data. Its objective is to establish the distinctiveness of a person based on immutable aspects of their anatomy or behavior. Biometric authentication relies on measuring physiological attributes or extracting behavioral patterns to ascertain identity, enabling recognition of individuals [7].

Physiological traits encompass various features like the iris, fingerprint, palm print, hand geometry, and facial characteristics. Meanwhile, behavioral attributes include voice, signature, gait, among other, as depicted in **Figure I.1**.

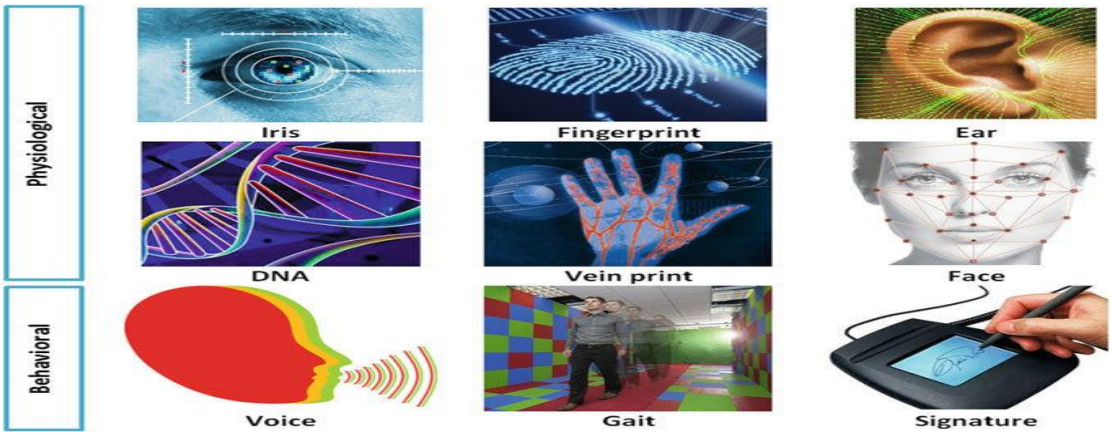

Figure I.1. Some biometric modalities

I.2 Various biometric modalities:

The diverse array of human biometric traits has led to the development of various authentication systems, each relying on a morphological, biological, or behavioral feature. Among these systems, certain ones have demonstrated reliability and have evolved over time. **Figure I. 2** depicts different biometric modalities utilized in various security and surveillance systems.

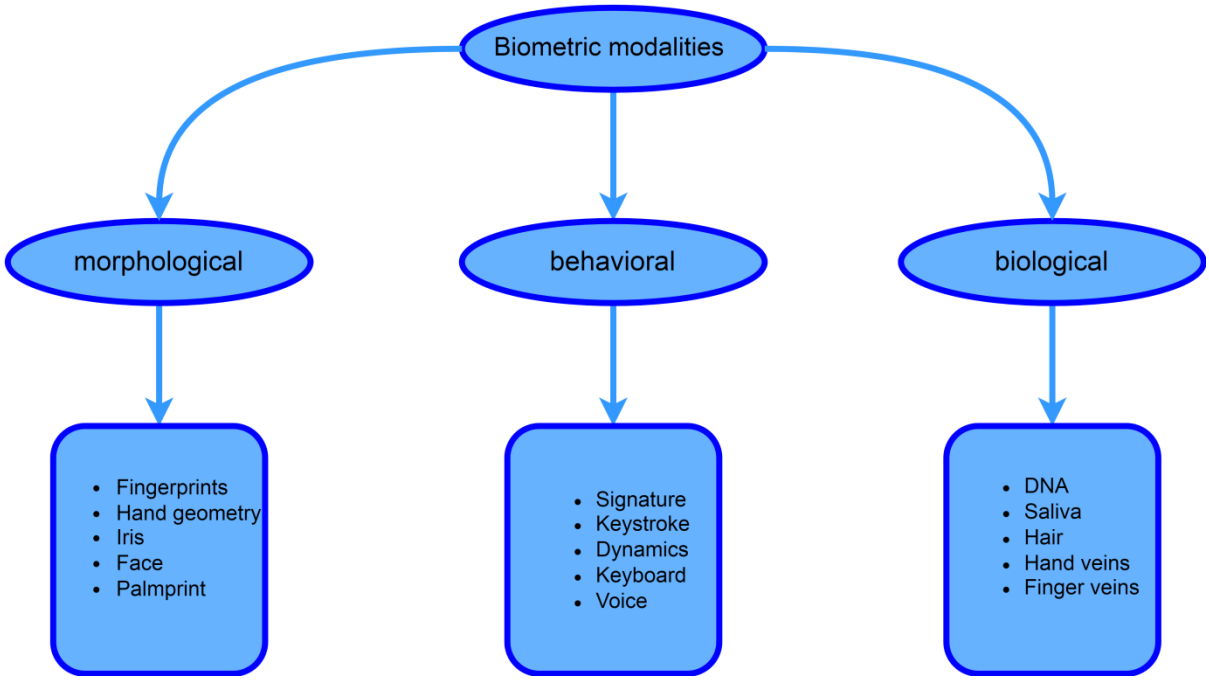

Figure I. 2. Categorization of various biometric modalities

I.2.1Palmprints:

The Palm print system is a manual biometric approach focusing on the inner surface of the hand, which shares similarities with fingertips but covers a larger area. Numerous features of a palm print can be utilized for individual identification. Palm prints offer more unique information compared to fingerprints. Additionally, palm print capture devices are more cost-effective than iris devices. They encompass distinct features like major wrinkles and creases, which can be extracted even from low-resolution images. **Figure I. 3** Illustrates the primary lines of the palm [8].

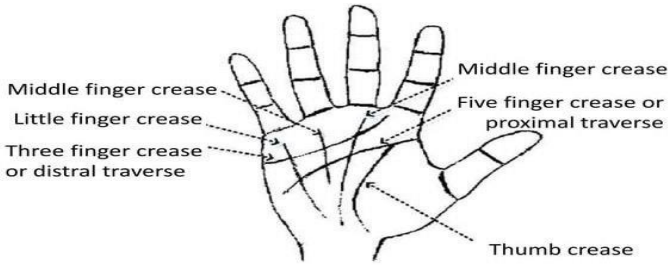

Figure I. 3. Definitions of palm lines and regions from scientists [9]

I.2.2 Finger knuckle print (FKP):

The Finger Knuckle Print (FKP) refers to the unique patterns formed by the ridges and grooves on the skin covering the finger joints. Unlike traditional fingerprints, FKP is often deemed a more reliable biometric modality due to its increased difficulty in replication or falsification. These prints are captured using a sensor and compared against a database for identity verification purposes. FKPs find common application in security systems for financial transactions and access to sensitive facilities [10]. **Figure I. 4**. depicts Finger Knuckle Prints (FKP).

Figure I. 4. Finger knuckle print (FKP)

I.2.3 Finger inner-knuckle print (FIKP):

The Finger Inner-Knuckle Print (FIKP) is an innovative hand biometric system that relies on finger knuckle patterns for identification. It introduces a refined extraction technique known as Average Local Line Binary Pattern (ALLBP) specifically tailored for finger knuckle patterns. This modality stands out by integrating minor and basic FIKP in a novel bimodal approach, a previously

unexplored concept. FIKP can serve as a standalone method for biometric recognition or be combined with other modalities to bolster security measures [11]. **Figure I.5** depicts the physiological characteristics of the inner finger region.

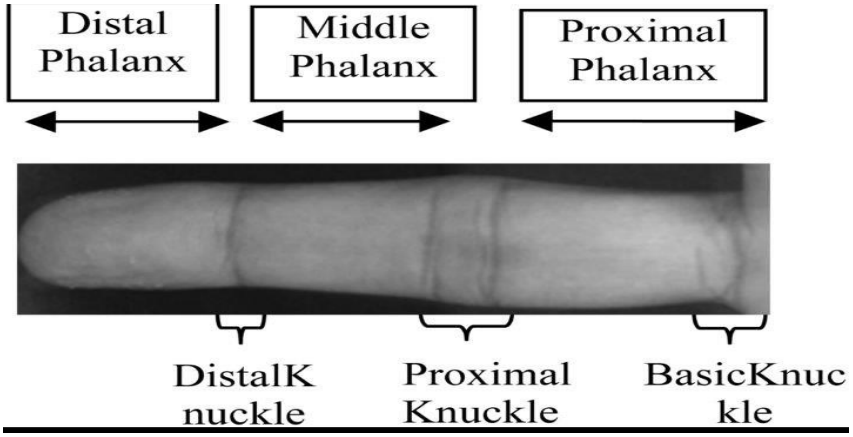

Figure I.5. Finger anatomy from an inner knuckle print surface (middle finger) [11]

I.2.4 Hand geometry:

This modality involves analyzing the shape of the hand, its length, width, height, and finger curvature, etc. This technique is recent, simple, and well accepted by users who follow sensor guides (infrared LEDs, digital cameras) to properly position their fingers, making detection/segmentation easier. However, this kind of system can be fooled by real twins or even by people with similar hand shapes. This technology offers a reasonable level of precision and is relatively easy to use. However, it can be easily deceived by twins or people with similar hand shapes [12]. **Figure I. 6** provides an illustration of hand geometry.

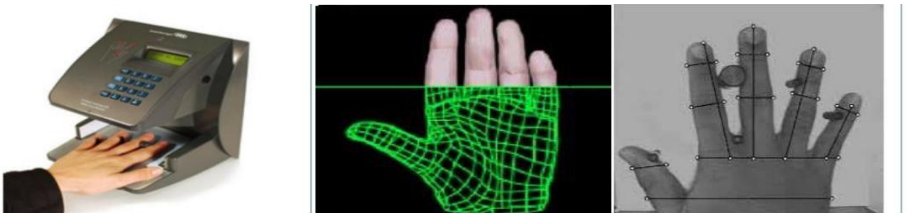

Figure I.6. Device for Recognizing Hand Geometry

I.2.5 Finger vein:

The veins of the fingers are hidden under the skin where red blood cells circulate. In biometrics, the term "vein" does not fully correspond to the terminology of medical science. Its network models are

used to authenticate a person's identity, in which the vein, about **0.3** to **1.0 mm** thick, is visible through near-infrared rays. In this definition, the term "finger" includes not only the index, middle, ring, and little fingers, but also the thumb. Finger-vein recognition [13] is one of the emerging biometrics and has been recently well studied. Compared to other biometric traits, the finger vein presents a higher degree of concealment and security in identification. Furthermore, compared to other vein recognitions, such as dorsal vein recognition [14], palm vein recognition [15], the size of the finger vein imaging device is smaller, and the credibility is higher. **Figure I. 7** below depicts finger veins captured in the near-infrared spectrum.

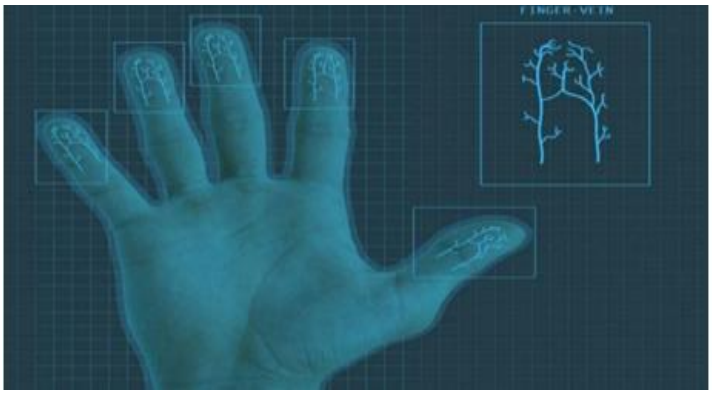

Figure I.7. Finger vein patterns [16]

I.2.6 Palm vein:

Palm vein authentication uses the vascular patterns of an individual's palm as personal identification data. Compared with a finger [17] or the back of a hand, a palm has a broader and more complicated vascular pattern and thus contains a wealth of differentiating features for personal identification. The palm is an ideal part of the body for this technology; it normally does not have hair which can be an obstacle for photographing the blood vessel pattern, and it is less susceptible to a change in skin color, unlike a finger or the back of a hand.

The deoxidized hemoglobin in the vein vessels absorb light having a wavelength of about 7.6 x10^{-4}mm within the near-infrared area [18]. When the infrared ray image is captured, unlike the image seen in **Figure I-8 (a),** only the blood vessel pattern containing the deoxidized hemoglobin is visible as a series of dark lines **Figure I-8 (b).** Based on this feature, the vein authentication device translates the black lines of the infrared ray image as the blood vessel pattern of the palm **Figure I-8 (c),** and then matches it with the previously registered blood vessel pattern of the individual.

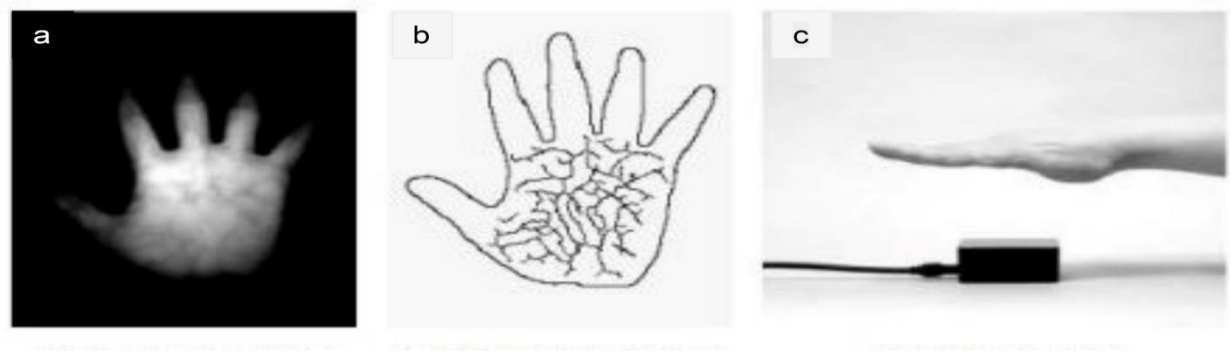

Figure I. 8: (a) Infrared ray image, (b) Extracted vein pattern, (c) Palm vein sensor

I.3 Architecture of biometric system:

The architecture comprises two main phases training and testing:

In the training phase, biometric data from an individual is collected and stored in a database. Typically, data captured by devices like security cameras or fingerprint readers is processed by a feature extraction module to isolate distinct traits. During recognition, data from a test subject is compared to stored data by a comparison module, with the decision module determining the individual's identity. Biometric systems can function in either verification or identification mode. See **Figure I. 9** for an illustration of the system.

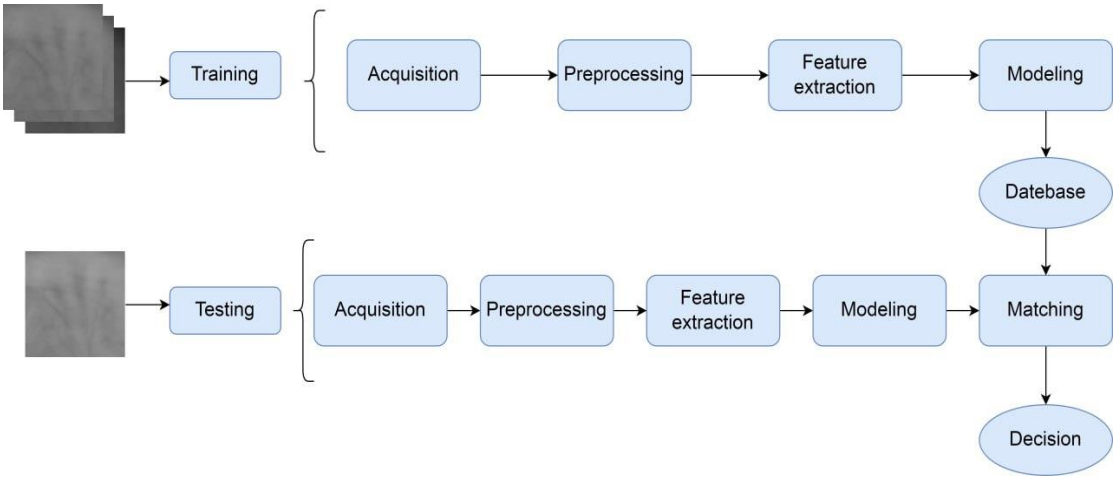

Figure I.9. Architecture of biometric system

I.3.1 Verification mode:

Verification mode in a biometric system is the process of confirming a user's identity by comparing captured biometric data with that stored in the database (see **Figure I. 10**). Typically, it proceeds as follows:

- Acquisition: The user submits their biometric data via a sensor, such as a hand and finger veins image.
- Biometric feature extraction: Image processing software analyzes the captured data, extracting specific characteristics crucial for identification.
- Matching module: Extracted biometric characteristics are then matched against stored templates in the database to determine if they correspond to an existing entry [19], refer for visual representation.

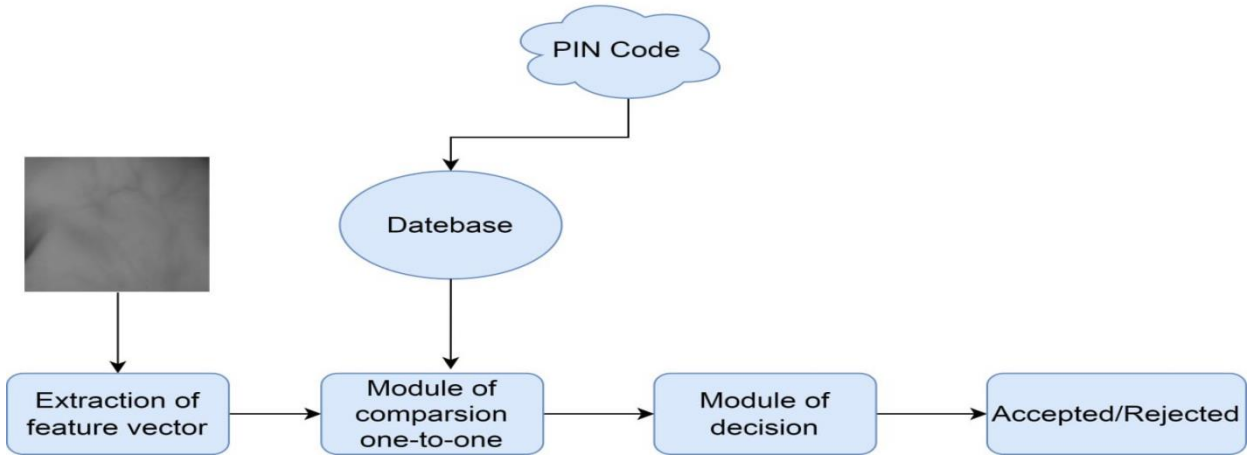

Figure I. 10. Flowchart of verification mode

I.3.2 Identification mode:

In identification mode, the user's identity isn't explicitly disclosed. Instead, the implicit assumption is that they belong to the pool of individuals already enrolled in the system. This scenario involves a 1: N match against the database. The biometric system's output provides the identity of the individual whose model shares the highest degree of similarity with the presented biometric sample. Typically, if the highest similarity score falls below a predetermined security threshold, the person is rejected, indicating that they aren't among the enrolled individuals. Conversely, if the similarity score exceeds the threshold, the person is accepted [20]. (Refer to **Figure I.11** for a visual depiction).

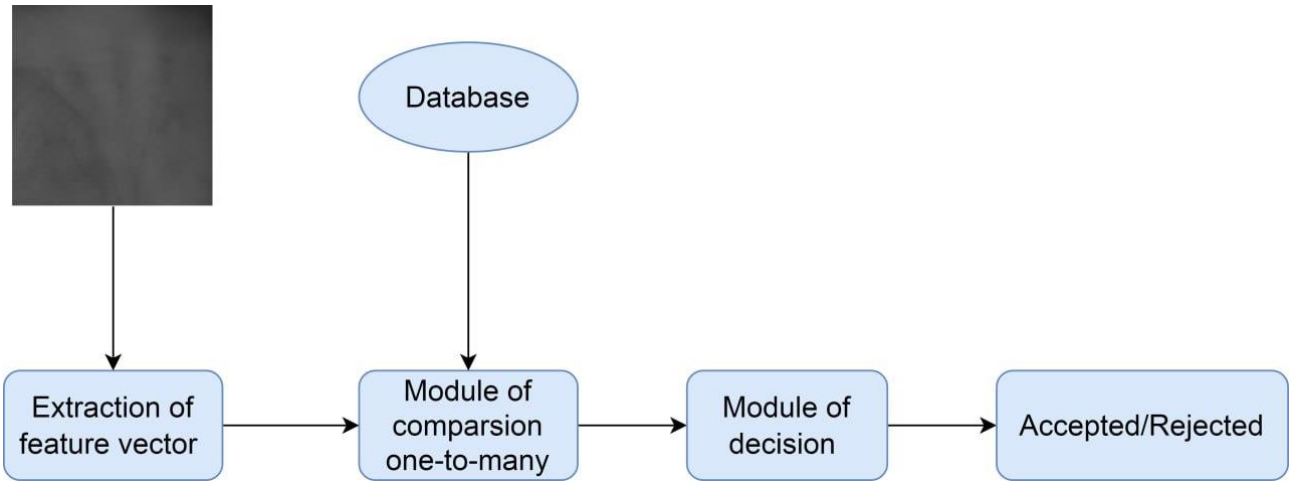

Figure I. 11. Flowchart of identification mode

I.4 Evaluation of a biometric system:

Evaluating a biometric system involves analyzing its performance to determine its quality and reliability. Important criteria for evaluating a biometric system include.

I.4.1 Identification mode:

The identification method within the biometric system integrates essential criteria for assessing verification system performance. These criteria directly impact the security level. The key criteria include the following:

I.4.1.1Speed: The time required to verify a person's identity is important in assessing the convenience of using the system.

I.4.1.2Recognition rate: is the ability of the system to correctly identify a person. Correct and incorrect recognition rates are important to evaluate the reliability of the system, In the context of biometric recognition systems operating in identification mode [21], Rank-1 is calculated by:

$$\mathbf{Rank-1} = \frac{\mathbf{N_i}}{\mathbf{N}} . \mathbf{100\%} \quad \mathbf{(1)}$$

With: **Ni** represents the number of images successfully assigned to the correct identity and **N** is the total number of images trying to assign an identity

I.4.1.3 CMC curve: The Cumulative Match Characteristic (CMC) curve is a widely used metric to evaluate the performance of biometric identification systems. It provides a graphical representation of the system's accuracy in identifying individuals within the top ranks of a candidate list [22]. **Figure I. 12** shows example of the CMC curve:

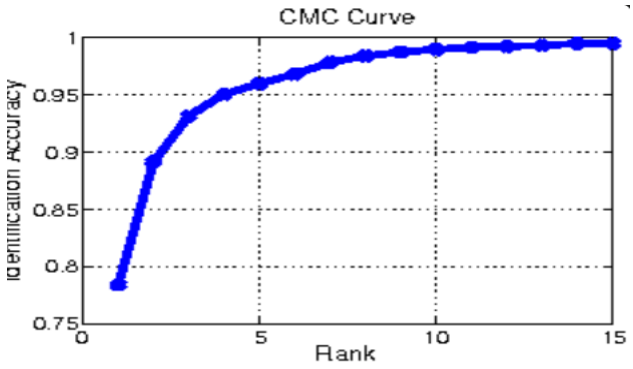

Figure I. 12. Example of the CMC curve [23]

I.4.2Verification mode:

The verification method in the biometric system includes fundamental measures for assessing the performance of verification systems. These measures directly impact both the security level and ease of use. The key measures include the following:

I.4.2.1FAR: "False Acceptance Rate" The False Acceptance Rate is a measure of the likelihood that the biometric system incorrectly accepts an unauthorized user. In the context of biometric authentication, the FAR represents the rate at which the system incorrectly identifies an unauthorized user as a legitimate one, leading to a false acceptance [24]:

$$\mathbf{FAR\ (T) = \frac{FA(T)}{N_i}} \qquad \mathbf{(2)}$$

With: **FA(T)** is the false acceptance rate and **Ni** the number of impostors in the base.

I.4.2.2 FRR: "False Reject Rate" The False Rejection Rate is a measure of the likelihood that the biometric system incorrectly rejects an authorized user. In the context of biometric authentication, the FRR represents the rate at which the system fails to recognize a legitimate user, leading to a false rejection [24] .

$$\mathbf{FRR\ (T) = \frac{FR(T)}{N_c}} \qquad \mathbf{(3)}$$

With: **FR(T)** is the False Rejection rate indicates the number of False Rejections and **NC** the number of customers in the database

I.4.2.3 EER: "Equal Error Rate" The third criterion is known as the Equal Error Rate (EER). The Equal Error Rate (EER) is the point at which the False Acceptance Rate (FAR) and False Reject Rate (FRR) are equal. This rate is also known as the crossover error rate. It serves as a crucial benchmark for evaluating the overall performance of a biometric system [24].

I.4.2.4 ROC curve: (Receiver Operating Characteristic) The Receiver Operating Characteristic (ROC) curve is extensively used to evaluate the performance of biometric systems by providing a graphical representation of the trade-off between the False Acceptance Rate (FAR) and the False Rejection Rate (FRR) at different operating points [25]. This curve can be broken down into three zones: high security zone, compromise zone and low security zone. **Figure I.13** show example of the ROC curve:

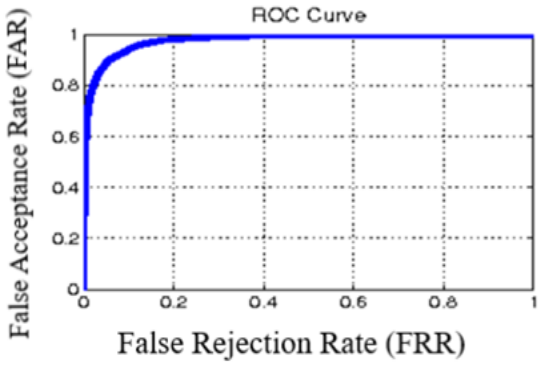

Figure I. 13. Example of the ROC curve

I.4.2.5 DET curve: The Detection Error Trade off (DET) curve is a graphical representation that shows the relationship between the False Reject Rate (FRR) and the False Acceptance Rate (FAR) in a biometric system. It is plotted parametrically based on the threshold values [26]. **Figure I.14.** shows example of the DET curve.

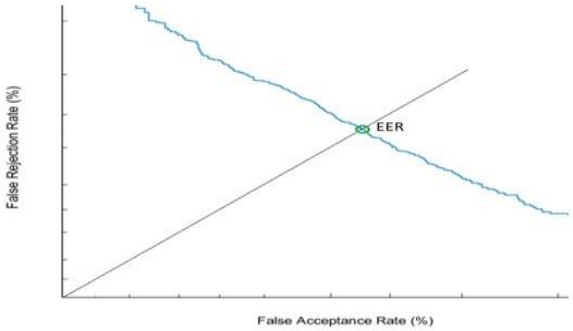

Figure I.14. Example of the DET curve

I.5 Multimodal biometric system:

A multimodal biometric system is an identity recognition system that uses multiple biometric modalities simultaneously to verify a person's identity, for example, a multimodal biometric system can use both fingerprints and retinal scanning to verify identity, as well as several fusion levels such as:

I.5.1 Fusion at the feature extraction level:

Fusion at the feature extraction level in a biometric system entails the direct amalgamation of data from diverse sensors or modalities at the onset of the processing phase. This form of fusion, often termed feature-level fusion, merges raw data from various biometric sources (see **Figure I. 15**). Subsequently, this unified feature vector is compared to an enrollment template, and a matching score is assigned, mirroring the procedure of a single biometric system [27].

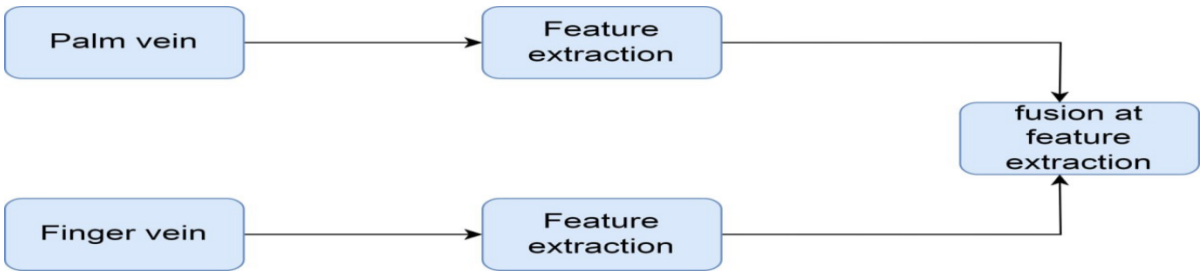

Figure I. 15. Fusion at feature extraction

I.5.2 Fusion at the score level:

Score-level fusion in multi biometric systems is a technique used to combine the scores generated by multiple biometric modalities, such as face and iris recognition, into a single score that is used to make a final decision about the identity of an individual (see **Figure I. 16**). This approach enhances the overall performance of the system by leveraging the strengths of each modality and mitigating the weaknesses [28].

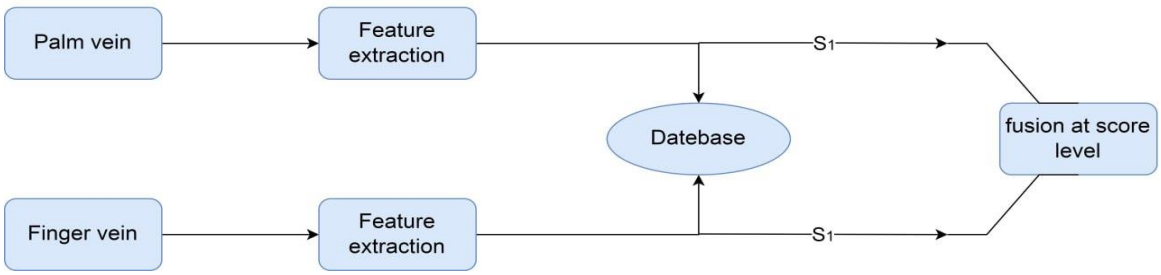

Figure I. 16. Fusion at score level

The different types of score-level fusion techniques used in biometric systems include:

We put Score $_{fusion}$ = (S_F) and Score$_1$= (S_1) also Score$_2$ = (S_2):

- ✧ **Simple-sum fusion technique:**

$$S_f = S_1 + S_2 \quad (4)$$

- ✧ **Min-score fusion technique:**

$$S_f = Min\,(S_1, S_2) \quad (5)$$

- ✧ **Max-score fusion technique:**

$$S_f = Max\,(S_1, S_2) \quad (6)$$

- ✧ **Matcher weighting fusion technique:**

$$S_f = W_1 \times S_1 + W_2 \times S_2 \quad (7)$$

Where:

$$W_1 + W_2 = 1 \quad (8)$$

The Weighted Sum is considered the most common in implementing the weighted schemes used in experiments for comparison and is given by the following equation [29]:

$$W_k = \frac{\frac{1}{EER_K}}{\sum_{k=1}^{k} \frac{1}{EER_K}} \quad (9)$$

These techniques are applied in score-level fusion to combine scores from multiple biometric modalities for enhanced verification and identification accuracy.

I.6 Application areas of biometrics:

Biometrics, which involves the use of unique physical or behavioral features for identification, has different applications across different sectors. Here are some of the main application areas of biometrics:

1. Law Enforcement and Public Security:

• Biometric systems support law enforcement agencies in criminal identification, utilizing technologies like Automated Fingerprint Identification Systems (AFIS) [30].

• Military agencies also use biometric data for identification purposes, such as collecting faces, irises, fingerprints, and DNA data [29].

2. Border Control, Travel, and Migration:

These systems enhance security measures at airports, borders, stadiums, and other sensitive locations [30].

3. Commercial applications:

Biometric systems are used in consumer and customer identification, particularly in retail stores They are also used in multi-factor authentication, combining biometric data with geolocation, IP addresses, and keying patterns to enhance security [30].

4. Legal applications:

Such as missing children, body identification, criminal investigation, terrorist identification, etc [31]

These applications demonstrate the versatility and importance of biometric technology in enhancing security measures, improving efficiency, and ensuring accurate identification across different sectors as shown by **Figure I.17**.

Figure I.17. Examples of application biometrics systems

Conclusion

In this chapter, we introduced the concept of biometric systems, their architecture and their different applications. We also noted that the performance of biometric systems depends on several factors and that it varies from one system to another. Among the criteria for evaluating the quality of the biometric system, we presented the equal error rates (EER), we also talked about multi-modal biometrics and its different type

Introduction:

As introduced in the first chapter, there are several biometric modalities applied in the field of identification and authentication. Among these modalities, we find that the palm print is a relatively new biometric. The recognition system for palm prints, like all biometric systems, consists of three essential steps: preprocessing, feature extraction, and classification. In this chapter, we will explain how to perform these steps using mathematical theory and discuss the objectives of the most commonly used methods in the research field.

II.1 State of the art in biometric system:

The state of the art in biometric systems involves the use of advanced technologies like machine learning and artificial intelligence to enhance security and accuracy in biometric recognition. Researchers are focusing on developing systems and algorithms that are resistant to spoofing attacks, ensuring the reliability of biometric authentication. Recent advancements have led to impressive results, with facial biometric systems achieving a 100% accuracy rate in identifying biometric attacks, along with high accuracy rates for iris and fingerprint recognition systems [32].

This progress signifies a significant step forward in the field of biometrics, emphasizing the importance of continuous innovation to address security challenges and improve authentication processes.

II.2 Identification/verification system:

The identification or verification system consists of three steps:

- Acquisition (database)
- Feature extraction (example: LPQ, Gabor,)
- Classification (example: SVM, KNN,)

II.2.1 Hand vein:

Hand veins, are a network of veins and blood vessels situated beneath the skin surface of the human hand. This intricate system of veins creates a distinct pattern of interconnected lines that is unique to each individual. These hand vein patterns serve as a physiological biometric trait that can be utilized for identification purposes, offering a secure and reliable method for personal verification [33]. It is possible to consider hand vein identification as the ability to recognize a unique individual through a suitable algorithm that exploits the characteristics of the vein. **Figure II. 1** illustrates some of the basic characteristics of hand veins.

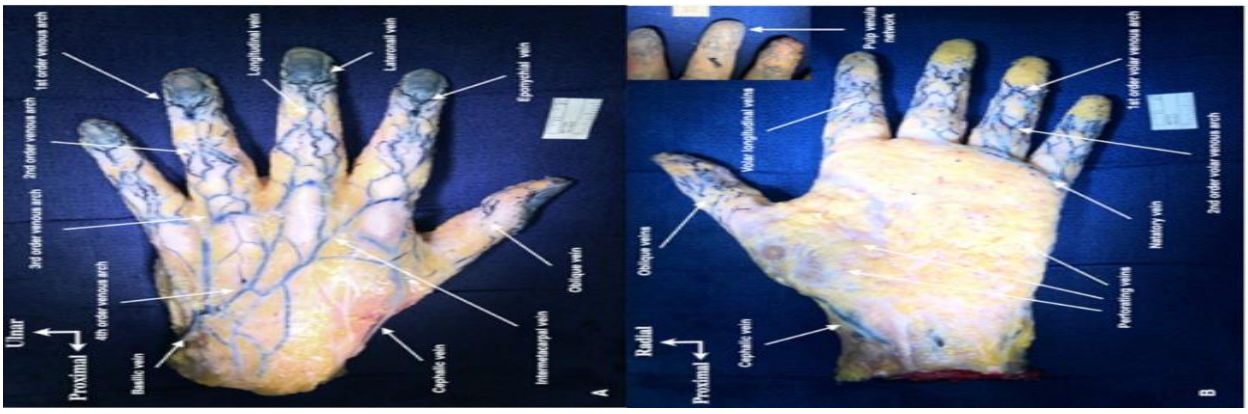

Figure II. 1. Some fundamental characteristics of the hand vein [34]

II.2.2Acquisition of the hand veins image:

The acquisition of hand vein images involves capturing images of the veins in the hand for various purposes like biometric identification and medical procedures. Different techniques are used for this process, including contactless methods that utilize near-infrared (NIR) light to make the vascular pattern visible. The acquisition devices are designed to optimize light source parameters based on image characteristics [35].

II.2.3The various methods in the state of the art for utilizing hand veins:

The paper "Personal Authentication Using Hand Vein Triangulation and Knuckle Shape" by Kumar and Prathyusha introduces a novel method for personal authentication utilizing hand vein images and knuckle shape data. The approach is automated and utilizes inexpensive, near-infrared, contactless imaging for acquiring palm dorsal hand vein images. Experimental results, based on a database of 100 users, demonstrate a low False Reject Rate of 1.14%, indicating a promising alternative for user identification [38]. The study conducted by Raghavendra, Mohammad Imran, Ashok Rao, and Kumar, G. H., titled "Multi-Modal Biometrics: Examination of Hand Vein and Palm Print Fusion for Personal Verification," investigates the fusion of hand vein and palm print

biometric data for personal verification purposes. Based on a database of 50 users, near-infrared, contactless imaging was used to acquire hand vein images. The approach utilizes two methodologies: Log Gabor transform and non-standard mask, demonstrating a low False Reject Rate of 4.8% and 1.4%, respectively.[39], The study conducted by Ferrer, M.A., Morales, A., Travieso, C.M., and Alonso, J.B., titled "Combining hand biometric traits for personal identification," is based on biometric features including hand geometry, palm and finger textures, and dorsal characteristics. Utilizing a database of 50 users, near-infrared, contactless imaging was employed. The approach utilizes the Simple Sum rule methodology, resulting in a low False Reject Rate and an equal error rate of 0.01% [40]. The query concerns the research conducted by YÜKSEL, Aycan; AKARUN, Lale; SANKUR, Bulent on "Biometric Identification through Hand Vein Patterns" . Utilizing a database of 100 users and near-infrared technology, the approach employs ICA 1, ICA 2, LEM, and NMF methodologies, resulting in low equal error rates of 5.4%, 7.24%, 7.64%, and 9.17% respectively [41]. In the research conducted by Wang, Y.D., Fan, Y., Liao, W.P., Li, K.F., Shark, L.K., and Varley, M.R., they introduced 'Hand vein recognition based on multiple key point sets.' In this paper, SIFT (Scale Invariant Feature Transform) was utilized for matching purposes. The proposed system reduced information redundancies, which were applied to a database of 2040 images, resulting in a high-performance recognition rate of 97.95%. The fusion of multiple sets of key points was proposed to identify the most reliable features [42]. Naidile, S. and Shrividya, G. conducted a study titled "Personal Recognition Based on Dorsal Hand Vein Pattern," focusing on the effectiveness of a hand vein biometric security system for authentication and identification. They proposed utilizing a NIR camera for capturing dorsal hand vein images and processing them through acquisition, preprocessing, feature extraction, and classification or matching stages. The paper highlights the use of maximum curvature for identifying vein centerlines post-preprocessing. The matching system employed a simple correlation method. Their database included right- and left-hand images of both male and female subjects. Experimental results showed a 75% positive detection rate and a 25% negative detection rate. They suggested further improvements by integrating additional recognition systems [43]. The research conducted by J. Cross and C. Smith, “Thermo graphic imaging of the subcutaneous vascular network of the back of the hand for biometric identification," employs a sequential correlation approach on vein signatures. It utilizes near-infrared, contactless imaging for acquiring hand vein images. Experimental results, based on a database of 20 hands, demonstrate a low False Reject Rate of 5.00% and a False Acceptance Rate of 0.00%, indicating a promising alternative for user identification [44]. A new personal verification system by TANAKA, Toshiyuki; KUBO, Naohiko. Based on a Biometric authentication by hand vein patterns., propose the certification system that

system compares vein images for low-cost, high-speed, and high-precision certification. The authentication equipment comprises a near-infrared light source and a monochrome CCD to produce contrast-enhanced images of the subcutaneous veins. We adopted phase-only correlation and template matching as recognition algorithms. Preliminary testing on a database containing 25 hands has been conducted, and the results are satisfactory, with an acceptable accuracy rate (FRR: 4.00% and FAR: 0.73%) [45]. A novel approach to personal verification by C. Lin and K. Fan, utilizing thermal images of palm-dorsal vein patterns, is presented in this paper. Our work employs a multi-resolution filter representation approach and an FIR camera for imaging. Testing on a database containing 32 hands has been conducted, and the results are satisfactory, with an acceptable accuracy rate (FRR: 2.3% and FAR: 2.3%). The experimental results demonstrate that our proposed approach is valid and effective for vein-pattern verification [46]. The paper by L. Wang and G. Leedham, titled "A thermal hand vein pattern verification system," utilizes (FIR) imagining, contactless imaging for acquiring palm dorsal hand vein images. This system directly recognizes the shapes of the vein pattern by measuring their Line-Segment Harsdorf Distance. Preliminary testing on a database containing 108 different images has been carried out, and all the images are correctly recognized [47]. In this paper, we begin by introducing the theoretical foundation and challenges of hand vein recognition. Subsequently, we delve into the study of threshold segmentation and thinning methods for hand vein images, proposing a new threshold segmentation method and an enhanced conditional thinning method. Additionally, we explore the method of hand vein image feature extraction based on end points and crossing points, followed by employing a matching method based on distances to match vein images. Utilizing near-infrared imaging, preliminary testing on a database containing 240 different images was conducted. The matching experiments indicated the efficiency of this method [48]. In this paper, we propose a new algorithm based on multi supplemental features and multi-classifier fusion decision, aiming to overcome the limitations of single-feature recognition. The approach utilizes near-infrared imaging. Preliminary testing was conducted on a database containing 500 different images. The experimental results indicate an acceptable accuracy rate (FRR: 5.00% and FAR: 0.00%) [49]. In this paper, two kinds of shape matching method are used, which are based on Harsdorf distance and Line Edge Mapping (LEM) methods. The vein image also contains valuable texture information, and Gabor wavelet is exploited to extract the discriminative feature. In order to evaluate the system performance, a dataset of 100 persons of different ages above 16 and of different gender, each has 5 images per person is used. Experimental results show that Hausdorff, LEM and Gabor based methods achieved 58%, 66%, 80% [50]. In this study, the authors present a novel hand vein database consisting of 300 images and a biometric technique based on the statistical processing of

hand vein patterns using Independent Component Analysis (ICA). The BOSPHORUS hand vein database was collected under realistic conditions where subjects underwent various procedures, such as holding a bag, pressing an elastic ball, and cooling with ice, all of which induce changes in vein patterns. The experimental results indicate an acceptable accuracy rate of 2.47% [51]. In this paper, we propose a novel approach: the Local Feature-Based Ensemble 2-Dimensional Linear Discriminate Analysis (LFBE-2D LDA) and 2D Principal Component Analysis (2D PCA), which utilizes a database of 4280 images and NIR imaging for dorsal hand vein recognition. This method uniquely combines local and global information, maximizing discriminate and descriptive image features. Experimental results on our extensive dorsal hand vein database demonstrate high accuracies (98.55%) achieved by our proposed method [52].

Table 1: Comparison of related works on hand vein-Based performance on different database

Reference	Methodology	Imaging	Database	Performance
Kumar, A., and Prathyusha, K.V [38]	Matching vein triangulation and shape features	Near IR imaging	100 Users	FAR = 1.14 FRR = 1.14
Raghavendra, R., Imran, M., Rao, A., and Kumar, G.H [39]	Log Gabor transform	Near IR imaging	50 users	FAR = 7.4, FRR = 4.8
	Non-standard mask			FAR = 2.8, FRR = 1.4
Ferrer, M.A., Morales, A., Travieso,C.M.and Alonso, J.B [40]	Simple Sum rule	Near IR imaging	50 users	FAR = 0.01, FRR = 0.01, EER = 0.01
Yuksel, A., and Akarun, L [41]	ICA 1, ICA2, LEM and NMF	Near IR imaging	100 users	EER =5.4, 7.24,7.64 and 9.17
YÜKSEL,Aycan; AKARUN, Lale [42]	SIFT(Scale Invariant Feature Transform)	Near IR imaging	2040 images,	Rank 1= 0.9795
AHMED,MonaA.; ROUSHDY,Mohamed; SALEM,Abdel-Badeeh M [43]	simple correlation method	Near IR imaging	Unknown	FAR = 0.75, FRR = 0.25
CROSS, J. M. SMITH [44]	sequential correlation approach on vein signatures	NearIR imaging	100 images	FAR = 0.00%, FRR = 5.00%
TANAKA,Toshiyuki, KUBO, Naohiko.[45]	fft phase correlation and template matching	Near IR imaging	25 hand	FAR = 0. 73%, FRR = 4.00%
LIN, Chih-Lung; FAN, Kuo-	multi-resolution filter	FIR	640 images	FAR = 2.30%,

Chin [46]	representation	imaging		FRR = 2.30%
WANG,Lingyu; LEEDHAM, Graham [47]	Line-Segment Hausdorff Distance	FIR imaging	108 images	FAR = 0.00,% FRR = 0.00%
DING,Yuhang; ZHUANG,Dayan; WANG, Kejun [48]	end points and crossing points	Near IR imaging	240 images	FAR = 0.00%, FRR = 0.90%
WANG, Kejun, et al [49]	multi supplemental features and multi-classifier fusion decision	Near IR imaging	500 images	FAR = 0.00%, FRR = 0.50%
WANG, Zhongli, et al [50]	Hausdorff distance and Line Edge Mapping(LEM)/ gabor	Near IR imaging	500 images	Rank 1= 0.6,0.8
YUKSEL,Aycan; AKARUN,Lale; SANKUR [51]	Independent Component Analysis (ICA)	Near IR imaging	300 images	Rank1= 0.94 FAR = 247% FRR = 2.47%
HSU, Chih-Bin, et al [52]	Block based on 2D LDA and 2D PCA	Near IR imaging	4280 images	Rank1= 0.99 FAR = 0.80%, FRR = 0.80%

II.2.4 Advantages and disadvantages of hand vein recognition:

Hand vein recognition, also known as vein pattern recognition, has its own set of advantages and disadvantages:

II.2.4.1The Advantages:

- **High Accuracy and Security:** Hand vein patterns are unique to each individual, providing a high level of accuracy for identification and authentication [53]
- **Biometric Stability:** Vein patterns remain relatively unchanged with age, ensuring consistent identification over a person's lifetime and reducing the need for frequent re-enrollment [53].
- **User-Friendly**: Capturing hand vein images is non-intrusive and generally comfortable, enhancing user acceptance and compliance [53].
- **Difficulty in Forgery:** Vein patterns are located beneath the skin, making them difficult to replicate or forge compared to other biometric modalities like fingerprints or facial recognition [53].

- **Hygienic and Contactless**: Modern systems can capture vein patterns without direct contact, promoting hygiene and reducing germ transmission, which is advantageous in public or shared spaces [53]

II.2.4.2The disadvantages:

- **Cost:** Hand vein recognition systems can be expensive to implement due to the advanced imaging technology required. This includes specialized infrared cameras and software capable of processing vein patterns [53].
- **Health-Related Issues:** Conditions such as severe dehydration, peripheral vascular disease, or hand injuries can affect vein visibility and recognition reliability [53].
- **Environmental Sensitivity**: Accuracy can be affected by environmental factors like lighting and temperature, which can impact image quality [53].

II.3The algorithms using in our proposed method:

II.3.1 Feature extraction:

Feature extraction constitutes one of the pivotal and essential steps in hand vein and finger vein recognition. In this phase, quantifiable characteristics of the fundamental biometric trait are generated, forming a model that is instrumental in individual identification. An effective feature extraction technique is a key factor in enhancing the accuracy of vein recognition.

II.3.1.1LPQ Method:

The LPQ (Local Phase Quantization) descriptor was initially proposed by Ojansivu and Heikkilä , The LPQ descriptor obtained is robust against centrally symmetric blur types like linear motion, out of focus, and atmospheric turbulence blur. The LPQ filter is designed to be blur-insensitive, making it suitable for texture analysis in images affected by various types of blur. It is based on the quantized phase information of the Fourier transform computed locally within image patches, providing a robust texture classification method [54].

The LPQ (Local Phase Quantization) operator is based on the concept of Time-Frequency (TF) analysis, specifically the Short-Time Fourier Transform (STFT). The LPQ operator uses Utilize the Short-Time Fourier Transform (STFT) to extract local phase information from an image, thereby focusing predominantly on phase details within the frequency domain, which is a prevalent technique in texture analysis [55].

In algorithms, the initial step involves transforming the image into representative features, a challenging task due to significant intra-class variations. Analyzing the blurring process could be formulated as [54]:

$$(\mathbf{x}) = (\mathbf{o} * \mathbf{h})(\mathbf{x}) \quad (10)$$

Where: b (x) is the observed image in the blurring process and o(x) is the original image , h(x) the point spread function (PSF) of the blur, Then, using the Fourier transform, this is converted to:

$$\mathbf{B(u)} = \mathbf{O(u)} \times \mathbf{H(u)} \quad (11)$$

If the Point Spread Function (PSF) h(x) exhibits central symmetry, it becomes real-valued and upholds the condition H(x) ≥ 0 in the low-frequency regions. The local Fourier coefficients are computed at four distinct frequency points [55]:

$$\mathbf{u_i(i = 1,..,4)}: \mathbf{u_1} = [\mathbf{a}, \mathbf{0}]^{\mathbf{T}}, \mathbf{u_2} = [\mathbf{0}, \mathbf{a}]^{\mathbf{T}}, \mathbf{u_3} = [\mathbf{a}, \mathbf{a}]^{\mathbf{T}}, \mathbf{u_4} = [\mathbf{a}, -\mathbf{a}]^{\mathbf{T}} \quad (12)$$

Where: a is a small scalar satisfying the condition H(x) > 0, resulting in four filtered images of both the real and imaginary parts of the transformation.

The **Figure II. 2**. shows the flowchart of all the necessary steps for the construction of the LPQ descriptor.

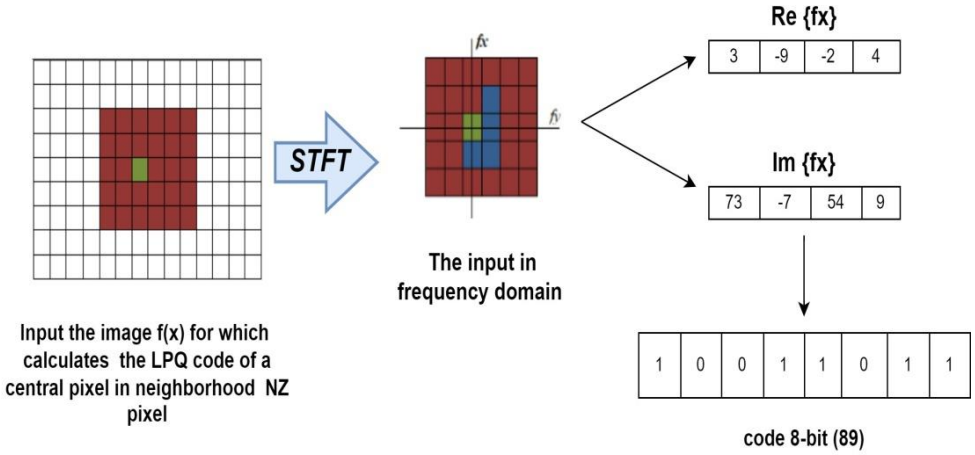

Figure II. 2. Principle of the LPQ Method

The LPQ features exhibit invariance to translation, rotation, and scale, making them resilient to changes in the image. Additionally, their implementation is relatively straightforward, adding to their practical appeal.

II.3.1.2 Gabor filter bank:

Gabor is a linear filter used in image processing for texture analysis, edge detection, and feature extraction. It is defined as the product of a Gaussian function modulated by an oriented sinusoidal plane wave. This modulation allows the filter to specifically respond to certain frequencies and orientations in an image, making it a useful tool for texture analysis and object detection [56].

Gabor filters are used for feature extraction in image analysis and computer vision but can introduce a DC component when the bandwidth is over one octave. Augmented Magnitude feature vector features are extracted using a Gabor filter bank, which consists of a family of 2D Gabor filters defined in the spatial domain [57].

$$\mathbf{Hu, v} = \frac{\mathbf{f_u^2}}{\boldsymbol{\pi n \lambda}} \mathbf{exp}\left[-\left(\frac{\mathbf{f_u^2}}{\mathbf{n^2}}\right)\mathbf{x_p^2} - \left(\frac{\mathbf{f_u^2}}{\boldsymbol{\lambda^2}}\right)\mathbf{y_p^2} \right] \mathbf{exp(j\, 2\pi\, f_u x_p)} \quad \textbf{(13)}$$

Where:

$$x_p = \mathbf{xcos}(\boldsymbol{\theta_v}) + \mathbf{ysin}(\boldsymbol{\theta_v}) \quad \textbf{(14)}$$

$$y_p = \mathbf{-xsin}(\boldsymbol{\theta_v}) + \mathbf{ycos}(\boldsymbol{\theta_v}) \quad \textbf{(15)}$$

$f_u = \frac{\text{fmax}}{2_2^u}$ and $\theta = \frac{\text{v}\pi}{8}$.

The principle behind the Gabor filter in biometric systems lies in its ability to enhance images, extract specific features, and improve the quality of biometric data for accurate recognition. The filter's mathematical properties and convolution process enable it to highlight relevant details in biometric images, making it a valuable tool in biometric identification and security system

II.3.2 Classification method:

Classification is an important task in machine learning that involves assigning a label to input data based on its characteristics. In other words, it is the process of finding a function that takes input features and produces an output label representing the category to which the data belongs.

There exist various classification methodologies, including supervised and unsupervised classification. In supervised classification, the model undergoes training on a dataset with predefined labels for each data point. Through supervised learning method like SVMs, neural networks, etc.

The model learns to correlate features with labels. On the other hand, unsupervised classification does not rely on labeled data for training; instead, it aims to group data based on their shared characteristics. Techniques like K-means, DBSCAN, etc., fall under unsupervised classification.

Classification finds applications across diverse domains such as image recognition, document classification, spam detection, biomedical signal classification, etc. [19].

- Choosing the data.
- Assessing similarities among n individuals using the initial dataset.
- Choosing and implementing a classification method.
- Analyzing and interpreting the outcomes.

II.3.2.1K-NN (k-Nearest Neighbors):

The k-Nearest Neighbors method, or k-NN for short, is a component of machine learning algorithms. Although the term "machine learning" was coined by American computer scientist Arthur Samuel in 1959, the concept itself is not novel. Machine learning algorithms experienced a notable resurgence in the early 2000s, primarily due to the proliferation of large datasets on the Internet.

In the k-Nearest Neighbors method, the task involves identifying, for each new individual requiring classification, the list of the k closest neighbors among the already classified individuals. Subsequently, the individual is assigned to the class containing the highest number of individuals among these nearest neighbors. The selection of the number of neighbors to consider is crucial. This method is non-parametric and supervised, often proving effective. Moreover, its learning process is relatively straightforward as it employs memory-based learning, retaining all training examples. However, prediction time is generally extended as it necessitates calculating distances with all examples, although there are heuristics available to streamline this process.

The principle behind this classification method is straightforward. It operates with a training dataset D, a distance function d, and an integer k. For each new test point x requiring a decision, the algorithm searches within D for the k points closest to x based on the distance d, then assigns x to the most common class among these k neighbors [58]. Refer to **Figure II. 3** for an illustration of the K-NN (k-Nearest Neighbors) method.

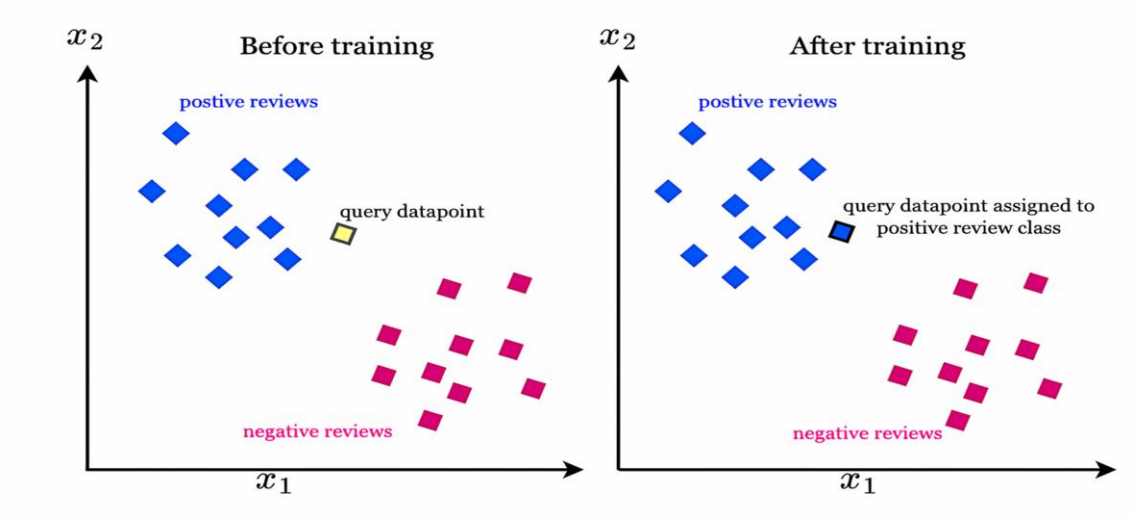

Figure II. 3: The K-NN Method

The image illustrates the concept of the K-NN (K-Nearest Neighbors) method, a classification algorithm in the field of machine learning. In the first graph titled "Before K-NN," there are data points representing two different classes, Class A and Class B, represented by different colors. A new data point that has not been classified yet is introduced. In the second graph titled "After K-NN," the K-NN method is used to classify the new data point. Based on its nearest K neighbors, the new data point is classified into Class B, as indicated by its color change to blue and the label indicating "New data point assigned to Class 1.

"The X1 and X2 axes represent the features or characteristics on which the method relies to determine the classification. The goal of K-NN is to classify new data based on similarity to existing data points.

❖ **The different Distance of K-NN:**

Most of the clustering method is based on the distance measures between data points. The large value of distance measure represents greater the difference between objects. The following are the most commonly used distance measures [59].

✧ **Euclidean distance:**

The Euclidean distance, also known as L2 norm, between two data point x_i and x_j is defined as:

$$D_e(x_i, x_j) = \left(\sum_{l=1}^{d} |x_{il} - x_{jl}|^2 \right)^{1/2} \quad (16)$$

Where : x_{il} and x_{jl} represent the l th dimension of xi and xj respectively. It tends to form hyperspherical clusters. The strength of this measure is that clusters formed are invariant to

translation and rotation in the feature space [60]. This measure has disadvantages also. If one of the input attributes has a relatively large range, then it can overcome the other attributes [61]

✧ **Manhattan distance:**

Manhattan distance also known as a city-block, rectilinear or L1 distance, is mathematically defined as:

$$D_{mn}(x_i, x_j) = \sum_{l=1}^{d} |x_{il} - x_{jl}|^2 \quad (17)$$

The clusters formed using Manhattan distance tend to form rectangular shaped clusters. Its advantage over Euclidean distance is the reduced computation time [62]. It does not depend upon the translation and reflection of the coordinate system. The one disadvantage is that it depends upon the rotation of the coordinate system.

✧ **Mahalanbois Distance:**

Mahalanobis introduced a new distance measure named as Mahalanobis distance [63]. It is based on the correlations between variables by which different patterns can be identified and analyzed. The squared Mahalanbois is defined as follows:

$$D_{ma}(x_i, x_j) = (x_i - x_j)V^{-1}(x_i - x_j)^T \quad (18)$$

where V is covariance matrix. It differs from the Euclidean distance in that it takes into account the correlations of the dataset. The Mahalanobis distance tends to form ellipsoidal clusters.

✧ **Cosine Distance:**

Cosine distance is a measure of similarity between two vectors by measuring the cosine of the angle between them. It is defined as:

$$D_{cos}(x_i, x_j) = 1 - \left(\frac{x_i^T x_j}{\|x_i\|\|x_j\|}\right) \quad (19)$$

It is used to measure cohesion within clusters [62]. It is also invariant to scaling. It is unable to provide information on the magnitude of the differences

✧ **Mahcos Distance:**

The Mahalanobis-Cosine (MAHCOS) distance can be applied to multivariate data by first applying the Mahalanobis distance to the multivariate data, then applying the Cosine distance to the results. This allows the application of the Mahalanobis-Cosine distance for analyzing multivariate data, enabling analysis of multivariate data while considering the similarity between variables [64].

❖ **how does the choice of k value affect the performance of k-nn method:**

The choice of the K value significantly impacts the performance of the K-Nearest Neighbors (KNN) algorithm. Here's how the K value affects the method performance:

- ✧ **Underfitting vs. Overfitting:** A smaller K value makes the model more sensitive to noise, potentially leading to overfitting. In contrast, a larger K value provides a smoother prediction but might lose detail, leading to underfitting.
- ✧ **Decision Boundary:** The K value influences the complexity of the decision boundary. Smaller K values result in more complex decision boundaries, capturing intricate patterns in the data. Larger K values lead to smoother decision boundaries, potentially oversimplifying the model.
- ✧ **Noise Sensitivity**: A small K value can make the algorithm sensitive to noise and outliers in the data,affecting the model's accuracy. On the other hand, a large K value may dilute local information, impacting the model's ability to distinguish between classes effectively.
- ✧ **Data Characteristics:** The optimal K value depends on the dataset's characteristics. Smaller K values are suitable for datasets with noise or complex decision boundaries, while larger K values are better for datasets with smoother decision boundaries.
- ✧ **Model Generalization:** The choice of K value affects the model's ability to generalize to unseen data. By experimenting with different K values and evaluating their impact on performance metrics like accuracy, the optimal K value can be determined for a specific dataset.

In summary, selecting the appropriate K value is crucial in balancing model complexity, noise sensitivity, and generalization capabilities to achieve optimal performance in the KNN algorithm [65].

II.3.2.2 Support Vector Machine (SVM):

SVM, short for Support Vector Machine, constitutes a family of machine learning algorithms capable of addressing classification, regression, or anomaly detection tasks. Renowned for their robust theoretical underpinnings, high adaptability, and user-friendly nature, SVMs can be effectively utilized even with limited knowledge of data exploration. They exhibit proficiency in handling both linear and nonlinear problems, proving beneficial across various practical applications. The fundamental concept behind SVM is straightforward: the method constructs a line or hyperplane to segregate the data into distinct classes.

SVM classifiers leverage the Optimal Hyperplane concept to determine a boundary between data points. By employing nonlinear functions, they map the data into the feature space, where an optimal hyperplane is established to partition the transformed data. The primary objective is to

construct a linear separation surface in the feature space, corresponding to a nonlinear surface in the input space [66].

How SVM Finds the Best Line:

According to the SVM method, we find the points closest to the line from both classes. These points are called support vectors. Next, we calculate the distance between the line and the support vectors, known as the margin. The goal is to maximize the margin. The hyperplane for which the margin is maximum is the optimal hyperplane. Therefore, SVM aims to create a decision boundary in a way that the separation between the two classes (this street) is as wide as possible (see **Figure II. 4**).

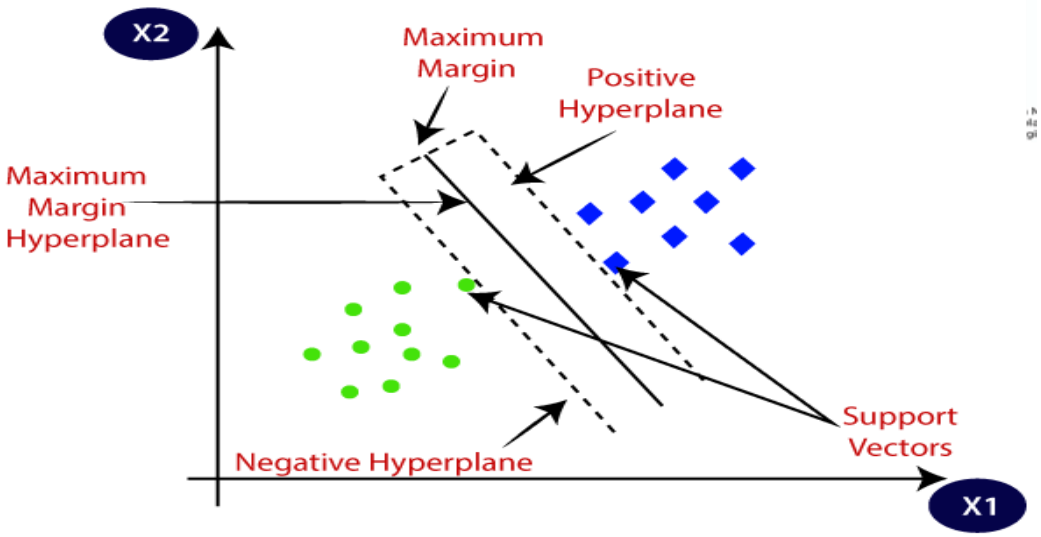

Figure II. 4: How SVM finds the bast line

❖ **The SVM approach involves two steps (see Figure II. 5):**

The SVM approach typically involves two main steps:

✧ **Training:** In this step, the SVM algorithm learns from a set of input-output training pairs to create the best decision boundary or hyperplane that separates the data points effectively. It identifies the support vectors that play a crucial role in defining the hyperplane.

✧ **Classification:** Once the SVM model is trained, it can be used for classification tasks where new data points are categorized into different classes based on the learned decision boundary. The SVM classifier uses the support vectors and the optimized hyperplane to classify new data points accurately [67].

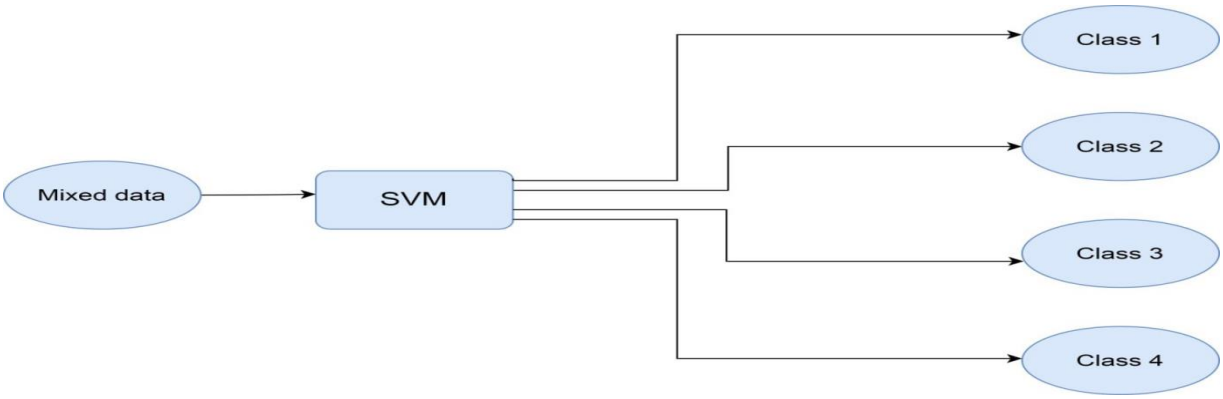

Figure II. 5: Principle of the SVM technique

Conclusion:

In conclusion, we were able to study the fundamental principle of vascular-based biometric identification system of the hand. This system consists of three steps. In the first step, the region of interest is extracted, which involves identifying the optimal section of the image for subsequent feature extraction. In the second step, in the feature extraction module, recognition systems undergo more significant steps before storing information in databases. There are several methods to perform this operation, such as LPQ and GABOR. In the final step, the data classification process groups similar features of one or more individuals into the same class. This step can be performed using methods such as KNN and SVM.

Introduction:

In this chapter, we will explore the process of identifying individuals through finger vein and palm vein recognition. We will discuss the various stages introduced in the previous chapter, utilizing MATLAB 2016. Additionally, we will introduce the experimental section, where we will present the results derived from our experiments

III.1 Database:

To evaluate the performance of our approach, we utilized data comprising two subsets: one for palmar finger veins and the other for palmar hand veins [68], totaling 42 subjects. Each subject contributed either 1 finger or 2 hands, with 5 images captured per finger or hand during a single session. Consequently, the finger vein subset consists of 210 images, while the hand vein subset comprises 840 images (with two illumination configurations at 850 nm and 950 nm, totaling 420 images each). The raw images, stored in 8-bit grayscale PNG format, have a resolution of 1280 × 1024 pixels. The visible area of the finger in the image's measures 600 × 180 pixels on average, while for the hand, it is approximately 750 × 750 pixels. Some sample images are depicted in **Figure III.1**.

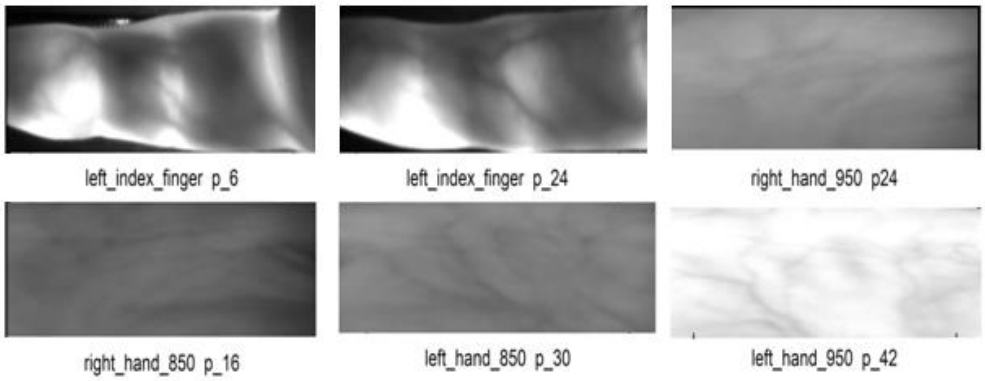

Figure III. 1: Some examples of databases

III.2 Extraction of the Region of Interest (ROI):

The main goal of region of interest (ROI) extraction is to choose the most appropriate part of an image for further feature extraction. This process also involves automatically normalizing the finger/hand region to prevent shifts, rotations, and accommodate scale changes. ROI extraction and finger/hand normalization are critical steps, particularly in contactless acquisition, to address the increased freedom of movement and various misplacements of fingers/hands. Various methods have been used for ROI extraction in both finger and hand vein images.

The finger vein images undergo alignment and normalization using a modified version of Lu et al.'s [69] method. This process ensures consistent finger positioning and width across images, despite varying finger placements. Initially, finger outlines are detected, and a centerline between them is established. The finger's centerline is then adjusted to the middle of the image through rotation and translation, masking out the regions outside the finger. Subsequently, the finger outline is normalized to a predefined width. Finally, a rectangular ROI (450 × 150 pixels) is extracted with its upper edge positioned at the fingertip.

The ROI method for hand vein images is based on Zhou and Kumar's [70] technique but is modified and expanded. Initially, the hand region is segmented by binarizing the image using local adaptive thresholding. Local minima and maxima points are then identified, where maxima correspond to finger tips and minima to finger valleys. For the palmar view and left hand, specific minima correspond to valleys between certain fingers. A line is fitted between these valley points, and the image is rotated to make this line horizontal. Subsequently, a square ROI is placed within the hand area, centered at the hand's center of mass, adjusted to the maximum size without including background pixels. Finally, the ROI image is scaled to 384 × 384 pixels. **Figure III.2** illustrates the steps to extract the region of interest (ROI) of finger and hand veins from the image.

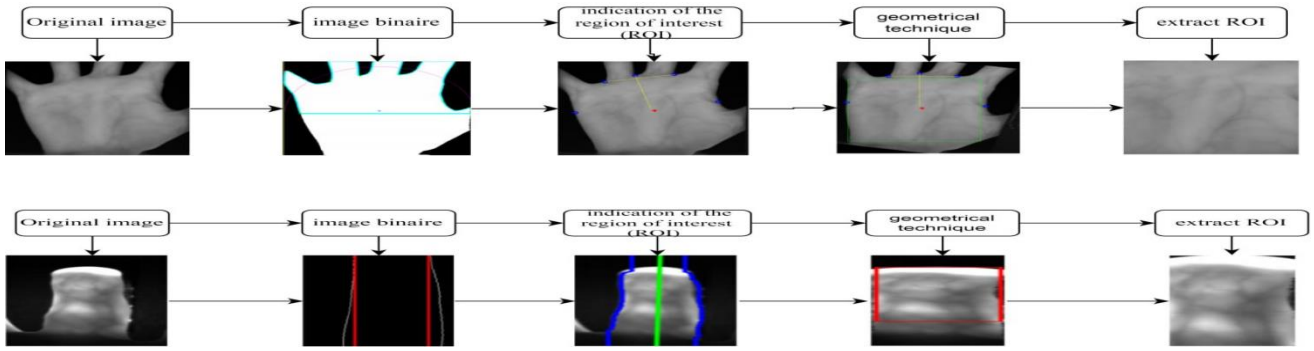

Figure III. 2: Steps for extracting the region of interest (ROI) for finger and hand veins

III.3 Results and discussion:

For system performance evaluation, we conducted a series of tests by comparing each pattern in the test images with all patterns in the reference dataset. If a pair of patterns belongs to the same user, we consider it a positive match, indicating the system's ability to correctly identify the user. Conversely, if the patterns belong to different users, we consider it a negative match, indicating a failure of the system to correctly identify the user.

The recognition rate was calculated by comparing the total number of positive matches with the total number of matches (both positive and negative). This protocol helps measure the accuracy of the system in recognizing images of hand veins and fingers and assessing its quality.

We applied our Gabor and LPQ algorithms to the reference database. The following tables provide a summary of the recognition rates obtained.

The VR@1FAR represents the verification rate at a 1% false acceptance rate (FAR), and the VR@0.1FAR represents the verification rate at a 0.1% false acceptance rate (FAR).

III.3.1The results were obtained using the LPQ method.

In this experiment, we utilized the LPQ filter for feature extraction of hand and finger veins. The results were obtained for different LPQ descriptor window sizes (Ws) and block sizes (Bs), which were varied to achieve the best results for identity verification and user recognition error rates. Finally, for the classification of the database, we used the K-NN algorithm with Mahcos distances

III.3.1.1Results of our method utilizing the left index finger:

Table 2: represents the identification and verification modes for LPQ filter scales for the left index finger, with a block size set to 100 and varying LPQ window sizes. The highest performance was achieved with a window size of 21. At this value, we obtained a Rank-1 recognition rate of 94.05% for the identification mode and an Equal Error Rate (EER) of 3.57% for the verification mode. Additionally, the verification rate at 1% FAR is 95.24%, and the verification rate at 0.1% FAR is also 95.24%. These results demonstrate the effectiveness of the LPQ filter with a window size of 21 for the feature recognition task studied in this experiment.

Table 2: Rank-1 /EER for different LPQ window sizes using the left index finger

WS	Identification	Verification		
	Rank 1(%)	EER (%)	VR@1FAR	VR@0.1FAR
3×3	82.14%	5.95%	86.90%	58.33%
5×5	88.10%	4.78%	90.48%	83.33%
7×7	88.10%	4.76%	92.86%	85.71%
9×9	94.05%	4.49%	95.24%	92.86%
11×11	94.05%	3.57%	95.24%	95.24%
13×13	92.86%	3.57%	95.24%	94.05%
15×15	91.67%	3.54%	95.24%	92.86%
17×17	91.67%	3.57%	95.24%	92.86%
19×19	92.86%	3.57%	95.24%	92.86%
21×21	94.05%	3.57%	95.24%	95.24%
23×23	94.05%	3.57%	95.24%	94.05%
25×25	94.05%	3.57%	95.24%	92.86%
27×27	94.05%	3.57%	95.24%	92.86%

Table 3: represents the identification and verification modes of the LPQ filter for the left index finger. Building upon the results outlined in Table 2, we fixed the window size at 21 and varied the block size, resulting in the following outcomes:

Table 3: Rank -1/EER for different LPQ Bloc size utilizing the left index finger.

Bs	Identification	Verification		
	Rank 1(%)	EER (%)	VR@1FAR	VR@0.1FAR
25×25	89.29%	4.86%	91.67%	84.52%
50×50	91.67%	4.78%	92.86%	88.10%
75×75	94.05%	4.76%	94.05%	90.48%
100×100	94.05%	3.57%	95.24%	92.86%
125×125	94.05%	4.78%	95.24%	92.86%
150×150	95.24%	3.57%	96.43%	94.05%
175×175	92.86%	3.57%	95.24%	92.86%
200×200	95.24%	3.57%	96.43%	94.05%
225×225	96.43%	3.56%	96.43%	96.43%
227×227	96.43%	3.56%	96.43%	96.43%
229×229	96.43%	3.57%	96.43%	95.24%

According to the results in Table 3, which indicate that the accuracy of recognition tests improves with an increase in block sizes, we have found that using a window size of 21 and a block size of 225 for the left index finger resulted in the highest Rank-1 recognition rate of 96.43%, with an Equal Error Rate (EER) of 3.56%. Additionally, the values of the verification rate at 1% FAR and the verification rate at 0.1% FAR indicate that the system can verify 96.43% of the samples at these false acceptance rates compared to other parameter values.

- The following **Figure III. 3** presents an example of the LPQ method applied to an image of the left Index finger with different parameter:

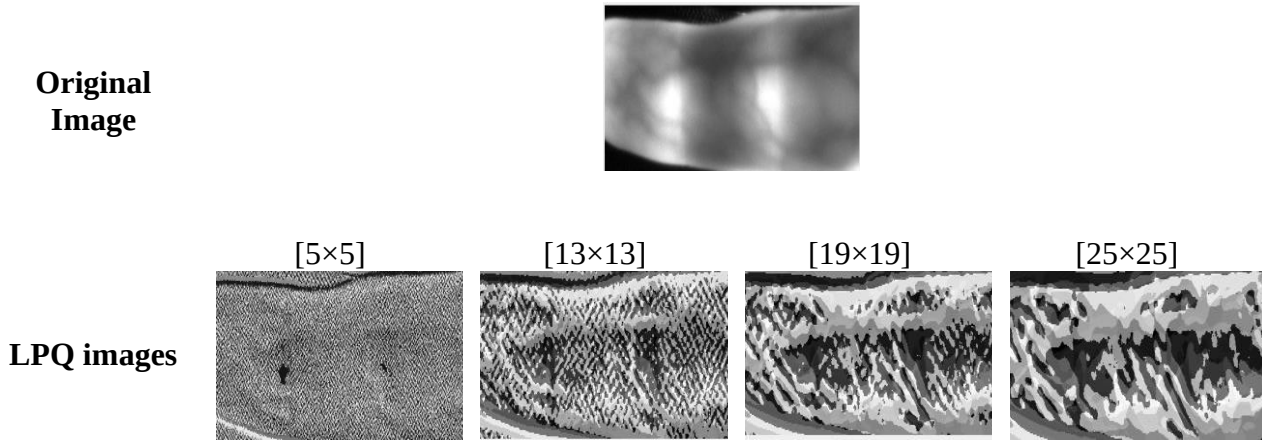

Figure III. 3: Example of the LPQ method applied to an image of the left Index finger

The images display the results obtained by applying the LPQ filter to the left index finger. We extracted the original image and other images taken under different parameters. We observed that the optimal visibility of the finger veins was attained when using a window size value of 25 compared to other values.

III.3.1.2Results of our method utilizing the right-hand vein 850:

Table 4: represents the identification and verification modes of the LPQ candidate for the right veins 850, evaluated with a block size set to 100 and varying LPQ window sizes. The highest performance was attained with a window size ranging from 15 to 27. Within this range, we achieved a Rank-1 recognition rate of 100.00% for the identification mode and an Equal Error Rate (EER) of 0.00% for the verification mode. Additionally, the verification rate at 1% FAR is 100.00%, and the verification rate at 0.1% FAR is also 100.00%.

Table 4: Rank -1/EER for different LPQ window sizes utilizing the right-hand vein 850

Ws	Identification	Verification		
	Rank 1(%)	EER (%)	VR@1FAR	VR@0.1FAR
3×3	91.67%	2.22%	95.24%	85.71%
5×5	98.81%	1.19%	98.81%	97.62%
7×7	98.81%	1.19%	98.81%	98.81%
9×9	98.81%	0.07%	100.00%	98.81%
11×11	98.81%	0.04%	100.00%	98.81%
13×13	98.81%	0.01%	100.00%	100.00%
15×15	100.00%	0.00%	100.00%	100.00%
17×17	100.00%	0.00%	100.00%	100.00%
19×19	100.00%	0.00%	100.00%	100.00%
21×21	100.00%	0.00%	100.00%	100.00%
23×23	100.00%	0.00%	100.00%	100.00%
25×25	100.00%	0.00%	100.00%	100.00%
27×27	100.00%	0.00%	100.00%	100.00%

Table 5: represents the identification and verification modes of the LPQ filter for the left index finger. Building up on the results outlined in Table 4, we fixed the window size at 15 and varied the block size, resulting in the following outcomes

Table 5: Rank -1/EER for different LPQ Bloc size utilizing the right-hand vein 850

Bs	Identification	Verification		
	Rank 1(%)	EER (%)	VR@1FAR	VR@0.1FAR
25×25	100.00%	0.01%	100.00%	100.00%
50×50	100.00%	0.00%	100.00%	100.00%
75×75	100.00%	0.00%	100.00%	100.00%
100×100	100.00%	0.00%	100.00%	100.00%
125×125	100.00%	0.00%	100.00%	100.00%
150×150	100.00%	0.00%	100.00%	100.00%
175×175	100.00%	0.00%	100.00%	100.00%
200×200	100.00%	0.00%	100.00%	100.00%
225×225	100.00%	0.00%	100.00%	100.00%

According to the results in Table 5, which also indicate that the accuracy of recognition tests improves with an increase in the number of block sizes, we have found that using a window size of 21 and a block size ranging from 50 to 225 for the right-hand vein led to the highest Rank-1 recognition rate of 100.00%, with an Equal Error Rate (EER) of 0.00%. Additionally, the values of the verification rate at 1% FAR and the verification rate at 0.1% FAR indicate that the system can verify 100.00% of both samples with high accuracy, indicating the effectiveness of the LPQ filter. This means that all users were correctly identified without errors.

- The following **Figure III. 4** presents an example of the LPQ method applied to an image of the right-hand vein 850 with different parameter:

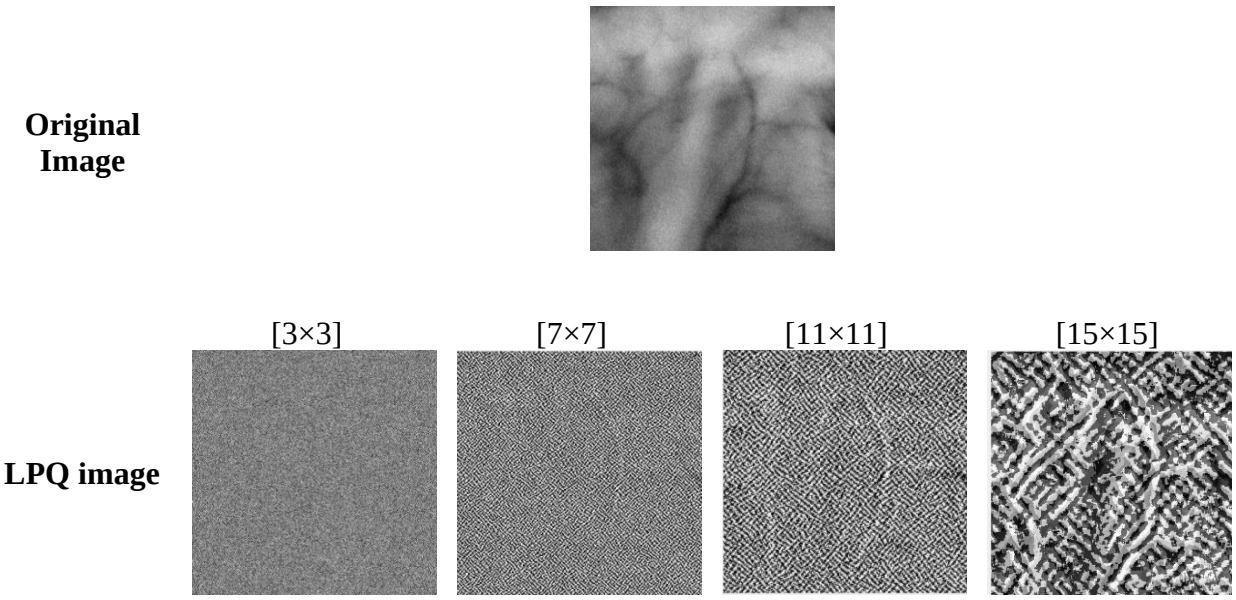

Figure III. 4: Example of the LPQ method applied to an image of the right-hand vein 850

The images display the results obtained by applying an LPQ filter to a right-hand vein at a wavelength of 850 nm. We extracted the original image along with additional images taken under different parameters. It was observed that optimal visualization of hand veins was achieved with a window size value of 15, surpassing other values. These results confirm the effectiveness of an LPQ filter with a block size of 15 for the feature recognition task investigated in this experiment.

III.3.1.3Results of our method utilizing the right-hand vein 950:

Table 6: represents the identification and verification modes of the LPQ candidate for the right veins 950, with a block size set to 100 and varying LPQ window sizes, which were evaluated. The highest performance was attained with a window size ranging from 7 to 27. Within this range, we achieved a Rank-1 recognition rate of 100.00% for the identification mode and an Equal Error Rate (EER) of 0.00% for the verification mode. Additionally, the verification rate at 1% FAR is 100.00%, and the verification rate at 0.1% FAR is also 100.00%

Table 6: Rank -1/EER for different LPQ window sizes utilizing the right-hand vein 950

Ws	Identification	Verification		
	Rank 1(%)	EER (%)	VR@1FAR	VR@0.1FAR
3×3	95.24%	1.19%	98.81%	85.71%
5×5	100.00%	0.07%	100.00%	97.62%
7×7	100.00%	0.00%	100.00%	100.00%
9×9	100.00%	0.00%	100.00%	100.00%
11×11	100.00%	0.00%	100.00%	100.00%
13×13	100.00%	0.00%	100.00%	100.00%
15×15	100.00%	0.00%	100.00%	100.00%
17×17	100.00%	0.00%	100.00%	100.00%
19×19	100.00%	0.00%	100.00%	100.00%
21×21	100.00%	0.00%	100.00%	100.00%
23×23	100.00%	0.00%	100.00%	100.00%
25×25	100.00%	0.00%	100.00%	100.00%
27×27	100.00%	0.00%	100.00%	100.00%

Table 7: presents the identification and verification modes of the LPQ filter for the finger. Building up on the results outlined in Table 6, we fixed the window size at 21 and varied the block size, resulting in the following outcomes:

Table 7: Rank -1/EER for different LPQ Bloc size utilizing the right-hand vein 950

Bs	Identification	Verification		
	Rank 1(%)	EER (%)	VR@1FAR	VR@0.1FAR
25×25	100.00%	0.00%	100.00%	100.00%
50×50	100.00%	0.00%	100.00%	100.00%
75×75	100.00%	0.00%	100.00%	100.00%
100×100	100.00%	0.00%	100.00%	100.00%
125×125	98.81%	0.09%	100.00%	95.24%
150×150	98.81%	0.07%	100.00%	98.81%
175×175	97.62%	0.12%	100.00%	97.62%
200×200	94.05%	3.37%	95.24%	90.48%
225×225	91.67%	3.59%	96.43%	79.76%

According to the results in Table 7, which also indicate that the accuracy of recognition tests improves with an increase in the number of block sizes, we have found that using a window size 7 and a block size ranging from 25 to 100 for the right-hand vein led to the highest Rank-1 recognition rate of 100.00%, with an Equal Error Rate (EER) of 0.00%. Additionally, the values of the verification rate at 1% FAR and the verification rate at 0.1% FAR indicate that the system can verify 100.00% of both samples with high accuracy, indicating the effectiveness of the LPQ filter. This means that all users were correctly identified without errors.

- The following **Figure III. 5** presents an example of the LPQ method applied to an image of the right-hand vein 950 with different parameter.

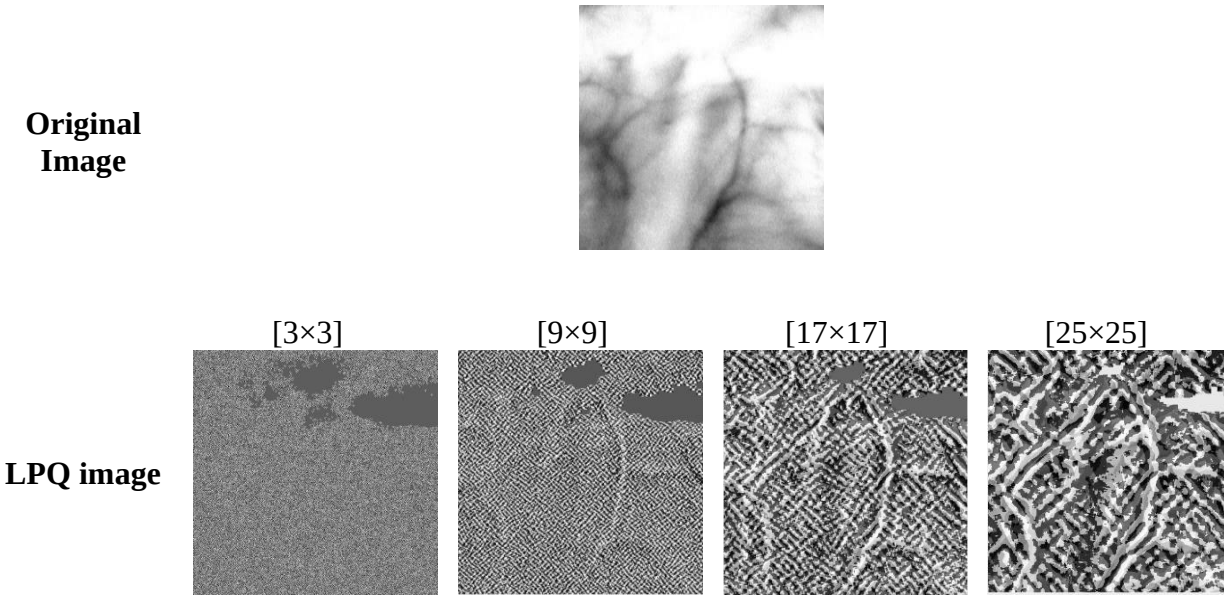

Figure III. 5: Example of the LPQ method applied to an image of the right-hand vein 950

The images display the results obtained by applying an LPQ filter to a right-hand vein at a wavelength of 950 nm. We extracted the original image along with additional images taken under different parameters. It was observed that optimal visualization of hand veins was achieved with a window size value of 25, surpassing other values. These results confirm the effectiveness of an LPQ filter with a block size of 25 for the feature recognition task investigated in this experiment.

III.3.1.4 Results of our method utilizing the left-hand vein 950:

Table 8: represents the identification and verification modes for LPQ filter scales for the left hand 950, with a block size set to 100 and varying LPQ window sizes. The highest performance was achieved with a window size of 25. At this value, we obtained a Rank-1 recognition rate of 98.81% for the identification mode and an Equal Error Rate (EER) of 0.93%for the verification mode. Additionally, the verification rate at 1% FAR is 100.00%, and the verification rate at 0.1% FAR is 98.81%. These results demonstrate the effectiveness of the LPQ filter with a window size of 25 for the feature recognition task studied in this experiment.

Table 8: Rank -1/EER for different LPQ window sizes utilizing the left-hand vein 950

Ws	Identification	Verification		
	Rank 1(%)	EER (%)	VR@1FAR	VR@0.1FAR
3×3	90.48%	4.76%	92.86%	79.76%
5×5	95.24%	3.57%	96.43%	92.86%
7×7	96.43%	2.38%	97.62%	95.24%
9×9	96.43%	2.38%	97.62%	95.24%
11×11	97.62%	1.18%	98.81%	97.62%
13×13	98.81%	1.19%	98.81%	98.81%
15×15	98.81%	1.19%	98.81%	98.81%
17×17	98.81%	1.19%	98.81%	98.81%
19×19	98.81%	1.19%	98.81%	98.81%
21×21	98.81%	1.19%	98.81%	98.81%
25×25	98.81%	0.93%	100.00%	98.81%
27×27	98.81%	1.06%	98.81%	98.81%

Table 9: represents the identification and verification modes of the LPQ filter for the left index finger. Building up on the results outlined in Table 8, we fixed the window size at 25and varied the block size, resulting in the following outcomes:

Table 9: Rank -1/EER for different LPQ Bloc size utilizing the left hand vein 950

Bs	Identification	Verification		
	Rank 1(%)	EER (%)	VR@1FAR	VR@0.1FAR
25×25	98.81%	0.09%	100.00%	98.81%
50×50	98.81%	0.96%	100.00%	98.81%
75×75	98.81%	1.19%	98.81%	98.81%
100×100	98.81%	0.93%	100.00%	98.81%
125×125	98.81%	0.19%	100.00%	98.81%
150×150	98.81%	1.19%	98.81%	98.81%
175×175	98.81%	1.19%	98.81%	98.81%
200×200	98.81%	1.19%	98.81%	98.81%
225×225	98.81%	1.18%	98.81%	98.81%

According to the results in Table 9, which also indicate that the accuracy of recognition tests improves with an increase in the number of block sizes, we have found that using a window size of 25 and a block size of 25 for the left-hand vein led to the highest Rank-1 recognition rate of 98.81%, with an Equal Error Rate (EER) of 0.09%. Additionally, the values of the verification rate at 1% FAR and the verification rate at 0.1% FAR indicate that the system can verify 100.00% and 98.81% of the samples at these false acceptance rates, respectively, compared to other parameter values.

- The following **Figure III. 6** presents an example of the LPQ method applied to an image of the left-hand vein 950 with different parameter:

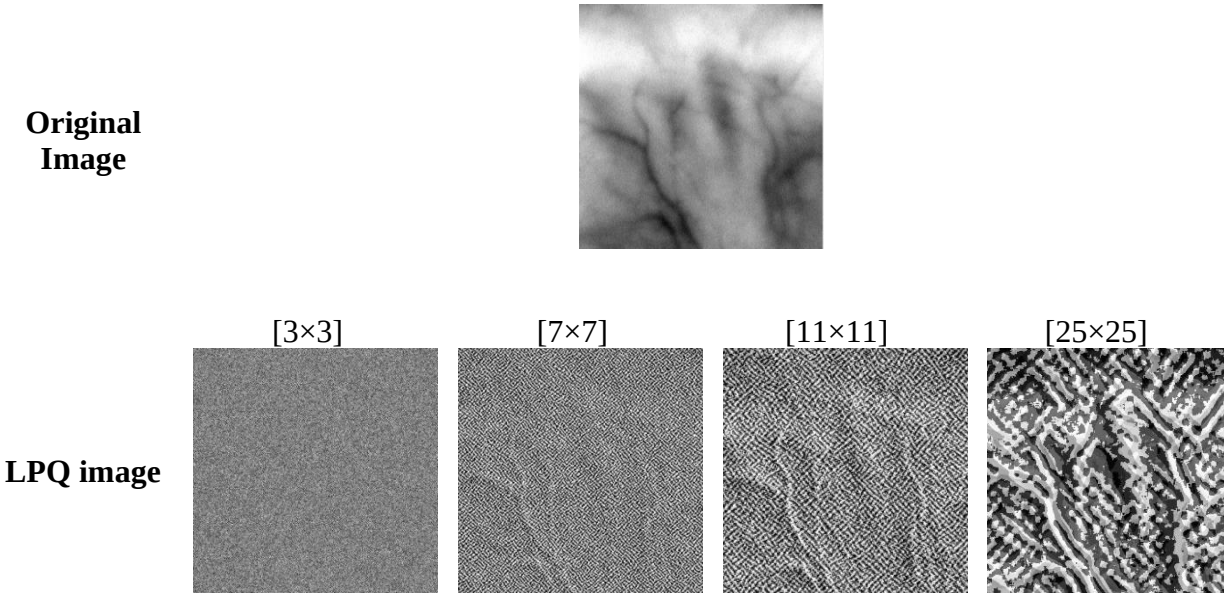

Figure III. 6: Example of the LPQ method applied to an image of the left-hand vein 950

The results shown demonstrate the effects of applying an LPQ filter to the left vein at a wavelength of 950 nm. In addition to the original image, other images taken under different parameters were obtained. It is worth noting that optimal visualization of hand veins was achieved with a window size of 25, superior to other options. These results highlight the efficiency of using an LPQ filter with a window size of 25 for the feature recognition task examined in this experiment.

III.3.1.5 Results of our method utilizing the left-hand vein 850:

Table10: represents the identification and verification modes for LPQ filter scales for the left hand 850, with a block size set to 100 and varying LPQ window sizes. The highest performance was achieved with a window size of 21. At this value, we obtained a Rank-1 recognition rate of 100.00% for the identification mode and an Equal Error Rate (EER) of 0.06% for the verification mode. Additionally, the verification rate at 1% FAR is 100.00%, and the verification rate at 0.1% FAR is 97.62%. These results demonstrate the effectiveness of the LPQ filter with a window size of 21 for the feature recognition task studied in this experiment.

Table 10: Rank -1/EER for different LPQ window sizes utilizing the left-hand vein 850

Ws	Identification	Verification		
	Rank 1(%)	EER (%)	VR@1FAR	VR@0.1FAR
3×3	89.29%	4.78%	90.48%	79.76%
5×5	94.05%	3.57%	94.05%	94.05%
7×7	94.05%	2.38%	96.43%	94.05%
9×9	96.43%	2.38%	97.62%	96.43%
11×11	96.43%	1.18%	97.62%	96.43%
13×13	98.81%	1.19%	98.81%	96.43%
15×15	96.43%	0.22%	100.00%	96.43%
17×17	96.43%	0.13%	100.00%	96.43%
19×19	98.81%	0.15%	100.00%	96.43%
21×21	100.00%	0.06%	100.00%	97.62%
25×25	98.81%	0.07%	100.00%	97.62%
27×27	98.81%	0.06%	100.00%	98.81%

Table 11: represents the identification and verification modes of the LPQ filter for the left index finger. Building upon the results outlined in Table 10, we fixed the window size at 21 and varied the block size, resulting in the following outcomes:

Table 11: Rank -1/EER for different LPQ Bloc size utilizing the left-hand vein 850

Bs	Identification	Verification		
	Rank 1(%)	EER (%)	VR@1FAR	VR@0.1FAR
25×25	97.62%	1.19%	98.81%	97.62%
50×50	98.81%	0.29%	100.00%	97.62%
75×75	98.81%	0.04%	100.00%	97.62%
100×100	100.00%	0.06%	100.00%	97.62%
125×125	100.00%	0.06%	100.00%	97.62%
150×150	97.62%	0.10%	100.00%	96.43%
175×175	98.81%	1.19%	98.81%	97.62%
200×200	100.00%	0.15%	100.00%	98.81%
225×225	100.00%	0.04%	100.00%	98.81%
227×227	100.00%	0.03%	100.00%	100.00%
229×229	100.00%	0.03%	100.00%	100.00%
300×300	97.62%	1.19%	97.62%	97.62%

According to the results in Table 11, which also indicate that the accuracy of recognition tests improves with an increase in the number of block sizes, we have found that using a window size of 21 and a block size of 227 for the left-hand vein 850 yields the highest Rank-1 recognition rate of 100.00%, with an Equal Error Rate (EER) of 0.03%. Additionally, the values of the verification rate at 1% FAR and the verification rate at 0.1% FAR indicate that the system can verify 100.00% of the samples at these false acceptance rates, respectively, compared to other parameter values.

- The following **Figure III. 7** presents an example of the LPQ method applied to an image of the left-hand vein 850 with different parameter:

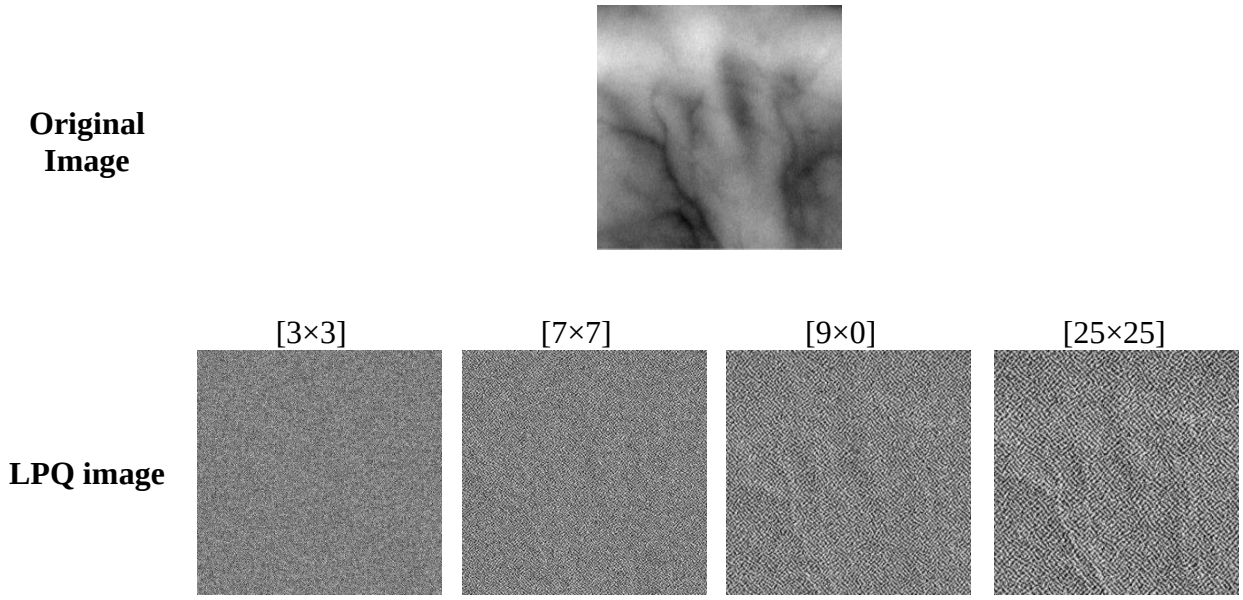

Figure III. 7: Example of the LPQ method applied to an image of the left-hand vein 850

The results demonstrate the impact of using an LPQ filter on the left vein at 850 nm. Along with the initial image, additional images under different parameters were acquired. Optimal visualization of hand veins was achieved with a window size of 25, These findings highlight the efficiency of using an LPQ filter with a window size of 25 for the feature recognition task examined in this experiment.

III.3.2The results were obtained using the GABOR filter bank:

In the following tables (12-21), we utilized the Gabor filter bank method to extract features for hand and finger veins. These tables exhibit the results obtained for various parameter values (number of orientations, number of scales, down sampling factor) using this method.

The tables present the results where the values of these parameters (number of orientations, number of scales, down sampling factor) were varied to attain the optimal results for identity verification and user recognition error rate.

Ultimately, for the classification of the database, we employed the K-NN algorithm with Mahcos distances.

III.3.2.1 Results of our method utilizing the left index finger:

Table 12: The illustration represents the Identification and Verification mode for the Gabor filter bank scales (with a fixed orientation value) for the left index finger. It demonstrates that increasing the number of scales generally results in improved system performance regarding recognition rate, error rate, VR@1% FAR, and VR@0.1% FAR.

The best results were attained when fixing the number of orientations at 2 and setting the down sampling factor to 64 bits. In this scenario, a Rank-1 recognition rate of 76.19% was achieved for identity recognition, with an Equal Error Rate (EER) of 7.13%. Additionally, the values of VR@1% FAR and VR@0.1% FAR indicate that the system can verify 77.38% and 63.10% of the samples, respectively, with high accuracy at scale 13.

Table 12: Rank -1/EER results of Gabor filter bank scales for the left index finger

Num_of_scales	Identification	Verification		
	Rank (%)	EER (%)	VR@1FAR	VR@0.1FAR
2	60.71%	14.29%	63.10%	34.52%
3	61.90%	13.10%	65.48%	36.90%
4	60.71%	11.92%	65.48%	38.10%
5	66.67%	11.90%	72.62%	50.00%
6	66.67%	10.71%	73.81%	45.24%
7	70.24%	10.71%	73.81%	50.00%
8	73.81%	9.52%	76.19%	52.38%
9	71.43%	9.80%	78.57%	54.76%
10	73.81%	9.52%	77.38%	60.71%
11	75.00%	8.33%	77.38%	64.29%
12	76.19%	8.13%	77.38%	65.48%
13	76.19%	7.13%	77.38%	63.10%
14	76.19%	8.13%	77.38%	65.48%

Table 13: The statement represents the Identification and Verification mode for Gabor filter bank scales (with a fixed scale value) for the left index finger. Based on the results presented in Table 12, we maintained the Gabor filter bank at scale 13 and the down sampling factor at 64 bits. In this scenario, we varied the orientation value, leading to the following outcomes.

Table 13: Rank -1/EER result Gabor filter bank of orientation the left index finger

Num_of_orient	Identification	Verification		
	Rank (%)	EER (%)	VR@1FAR	VR@0.1FAR
3	80.95%	8.33%	83.33%	65.48%
4	84.53%	8.35%	88.10%	70.24%
5	88.10%	7.13%	90.48%	76.19%
6	85.71%	5.95%	91.67%	78.57%
7	88.10%	5.95%	91.67%	77.38%
8	86.90%	5.95%	91.67%	77.38%
9	86.90%	5.97%	91.67%	76.19%
10	86.90%	5.95%	90.48%	75.00%

According to the results in Table 13, which also indicate that the accuracy of recognition tests improves with an increase in the number of orientations, we found that using a Gabor filter bank with 13 scales, an orientation factor of 7, and a fixed down sampling factor of 64 bits for the left index finger resulted in the highest Rank-1 recognition rate of 88.10%, with an Equal Error Rate (EER) of 5.95%. Additionally, the values of VR@1% FAR and VR@0.1% FAR indicate that the system can verify 91.67% and 77.38% of the samples, respectively, compared to other orientation parameter values.

- The following **Figure III. 8** presents an example of the Gabor filter bank applied to an image of the left index Finger with different parameter:

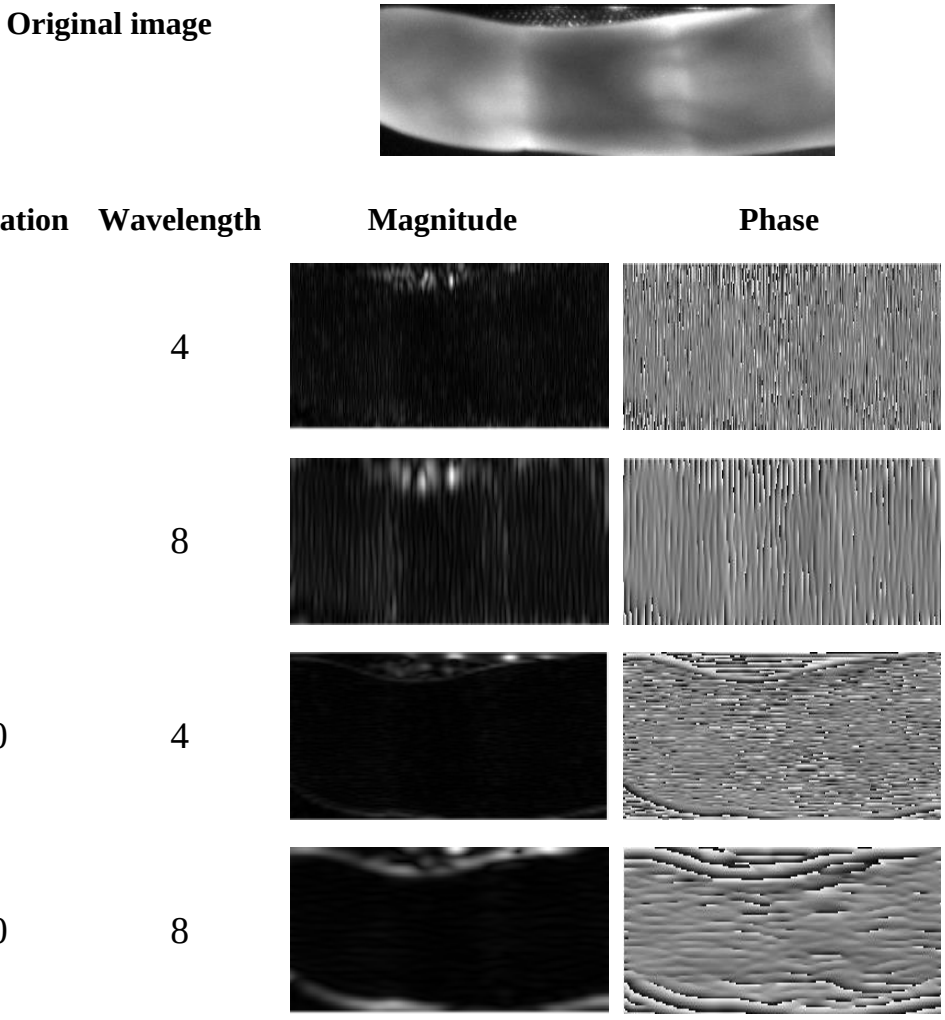

Figure III. 8: Example of the Gabor filter bank applied to an image of the left index finger

III.3.2.2 Results of our method utilizing the right-hand vein 850

Table 14: The passage represents the Identification and Verification mode for Gabor filter bank scales (with a fixed orientation value) using the right-hand veins (specifically, right hand vein 850). It demonstrates that increasing the number of scales significantly enhances the system's performance in terms of recognition rate, error rate, VR@1% FAR, and VR@0.1% FAR. The best results were achieved with the orientation number fixed at 2 and the down sampling factor set to 64 bits. In this case, a Rank-1 recognition rate of 100.00% was achieved for identity verification, with an Equal Error Rate (EER) of 0.01%. Additionally, the values of VR@1% FAR and VR@0.1% FAR indicate that the system can verify 100.00% of the samples with high accuracy at scale

Table 14: Rank -1/EER results of Gabor filter bank scales for right hand vein 850

Num_of_scales	Identification	Verification		
	Rank (%)	EER (%)	VR@1FAR	VR@0.1FAR
2	45.24%	19.05%	44.05%	14.29%
3	46.43%	14.27%	47.62%	13.10%
4	53.57%	11.00%	63.10%	33.33%
5	82.14%	4.76%	84.52%	57.14%
6	94.05%	1.05%	100.00%	84.52%
7	97.62%	0.01%	100.00%	100.00%
8	100.00%	0.01%	100.00%	100.00%
9	100.00%	0.03%	100.00%	100.00%
10	100.00%	0.01%	100.00%	100.00%
11	100.00%	0.03%	100.00%	100.00%

Table 15: The passage represents the Identification and Verification mode for Gabor method scales (with a fixed scale value) for the right-hand veins (specifically, right hand vein 850). Based on the results presented in Table 14, we maintained the Gabor filter bank at scale 10 and the down sampling factor at 64 bits. In this case, we varied the orientation value, resulting in the following outcomes:

Table 15: Rank -1/EER results of Gabor filter bank orientation for right hand vein 850

Num_of_orient	Identification	Verification		
	Rank (%)	EER (%)	VR@1FAR	VR@0.1FAR
3	100.00%	0.00%	100.00%	100.00%
4	100.00%	0.00%	100.00%	100.00%
5	100.00%	0.00%	100.00%	100.00%
6	100.00%	0.00%	100.00%	100.00%
7	100.00%	0.00%	100.00%	100.00%
8	100.00%	0.00%	100.00%	100.00%
9	100.00%	0.00%	100.00%	100.00%
10	100.00%	0.00%	100.00%	100.00%

According to the results in Table 14, which indicate that the accuracy of recognition tests improves with an increase in the number of orientations, we found that using a Gabor filter bank with 10 scales, an orientation factor of 3 or above, and a fixed down sampling factor of 64 bits for the right-hand vein 850 yielded the highest Rank-1 recognition rate of 100.00%, with no Equal Error Rate (EER). Additionally, the values of VR@1% FAR and VR@0.1% FAR indicate that the system can verify 100.00% of both samples with high accuracy, indicating the effectiveness of the Gabor filter bank. This means that all users were correctly identified without errors.

- The following **Figure III. 9** presents an example of the Gabor filter bank applied to an image of the right-hand veins _850 with different parameter:

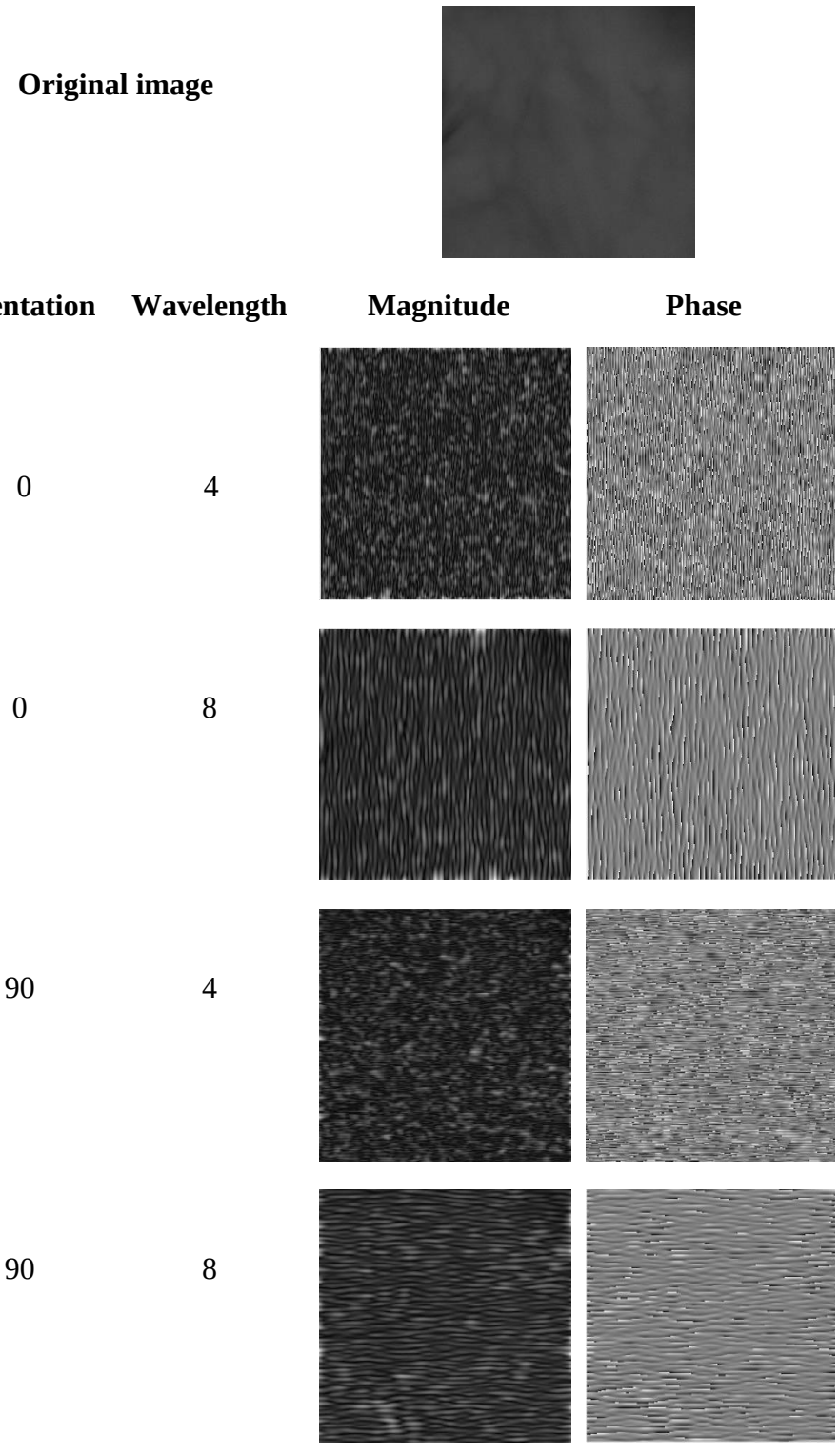

Figure III. 9: Example of the Gabor filter bank applied to an image of the right-hand vein 850

III.3.2.3Results of our method utilizing the right-hand veins 950

Table 16: represents the Identification and Verification mode for Gabor filter bank scales (with fixed orientation values) using the right-hand vein 950, showing that increasing the number of scales led to a significant improvement in system performance in terms of recognition rate, error rate, VR@1% FAR, and VR@0.1% FAR. The best results were achieved when fixing the number of orientations at 2 and setting the down sampling factor to 64 bits. In this case, a Rank-1 recognition rate of 100.00% was achieved for identity recognition, with an Equal Error Rate (EER) of 0.03%. Additionally, VR@1% FAR and VR@0.1% FAR values indicate that the system can verify 100.00% of both samples with high accuracy at scales 9 and 10.

Table 16: Rank -1/EER results of Gabor filter bank scales for right hand vein 950

Num_of_scales	Identification	Verification		
	Rank (%)	EER (%)	VR@1FAR	VR@0.1FAR
2	42.86%	19.92%	44.05%	5.95%
3	52.38%	17.84%	50.00%	11.90%
4	66.67%	10.71%	60.71%	25.00%
5	78.57%	3.70%	84.52%	40.48%
6	91.67%	2.38%	97.62%	83.33%
7	92.86%	1.19%	97.62%	96.43%
8	98.81%	0.09%	100.00%	97.62%
9	100.00%	0.03%	100.00%	100.00%
10	100.00%	0.03%	100.00%	100.00%

Table 17: represents the identification and verification mode for Gabor filter bank scales (with a fixed scale value) for the right-hand vein 950 based on the results found in Table 16. We fixed the Gabor filter bank at scale 10 and the down sampling factor at 64 bits. In this case, we varied the orientation value, resulting in the following outcomes:

Table 17: Rank -1/EER results of Gabor filter bank orientation for right hand vein 950

Num_of_orient	Identification	Verification		
	Rank (%)	EER (%)	VR@1FAR	VR@0.1FAR
3	100.00%	0.00%	100.00%	100.00%
4	100.00%	0.00%	100.00%	100.00%
5	100.00%	0.00%	100.00%	100.00%
6	100.00%	0.00%	100.00%	100.00%
7	100.00%	0.00%	100.00%	100.00%
8	100.00%	0.00%	100.00%	100.00%
9	100.00%	0.00%	100.00%	100.00%
10	100.00%	0.00%	100.00%	100.00%

According to the results in Table 17, it is evident that the accuracy of recognition tests improves with an increase in the number of orientations. We also found that using a Gabor filter bank with 10 scales, an orientation factor of 3 or above, and a fixed down sampling factor of 64 bits for the right-hand vein 850 resulted in the highest Rank-1 recognition rate of 100.00%, with an absence of Equal Error Rate (EER). Additionally, VR@1% FAR and VR@0.1% FAR values indicate that the system can verify 100.00% of both samples with high accuracy, highlighting the effectiveness of the Gabor filter bank. This means that all users were correctly identified without errors.

- The following **Figure III. 10** presents an example of the Gabor filter bank applied to an image of the right-hand vein 950 with different parameter:

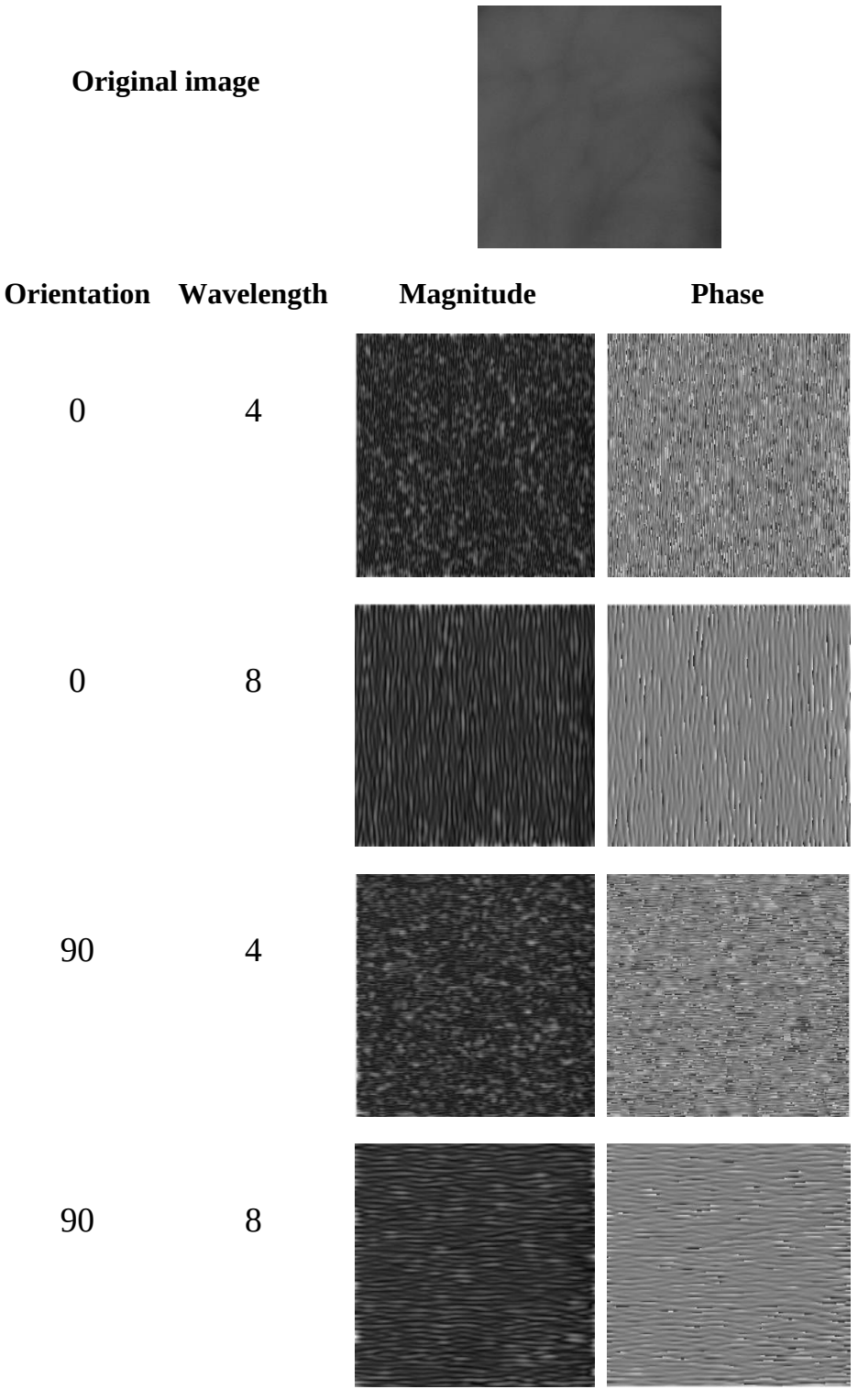

Figure III. 10: Example of the Gabor filter bank applied to an image of the right-hand vein 950

III.3.2.4 Results of our method utilizing the left-hand vein 950

Table 18: represents the Identification and Verification mode for Gabor filter bank scales (with a fixed orientation value) using the left-hand vein 950. It shows that increasing the number of scales significantly improves the system's performance in terms of recognition rate, error rate, VR@1% FAR, and VR@0.1% FAR. The best results were achieved when fixing the number of orientations at 2 and setting the down sampling factor to 64 bits. In this case, a Rank-1 recognition rate of 96.43% was achieved for identity recognition, with an Equal Error Rate (EER) of 0.26%. Additionally, VR@1% FAR and VR@0.1% FAR values indicate that the system can verify 100.00% and 95.24% of the samples respectively with high accuracy at scale 9.

Table 18: Rank -1/EER results of Gabor filter bank scales for left hand vein 950

Num_of_scales	Identification	Verification		
	Rank (%)	EER (%)	VR@1FAR	VR@0.1FAR
2	30.95%	19.21%	32.14%	5.95%
3	41.67%	16.65%	39.29%	8.33%
4	66.67%	11.90%	60.71%	33.33%
5	83.33%	4.76%	84.52%	53.57%
6	91.67%	3.28%	96.43%	79.76%
7	95.24%	1.42%	97.62%	92.86%
8	96.43%	1.20%	97.62%	94.05%
9	96.43%	0.26%	100.00%	95.24%
10	96.43%	1.03%	100.00%	95.24%

Table 19: represents the identification and verification mode for Gabor filter bank scales (with a fixed scale value) for the left-hand vein 950 based on the results found in Table 18. We fixed the Gabor filter bank at scale 9 and the down sampling factor at 64 bits. In this case, we varied the orientation value, resulting in the following outcomes:

Table 19: Rank -1/EER results of Gabor filter bank orientation for left hand vein 950

Num_of_orient	Identification	Verification		
	Rank (%)	EER (%)	VR@1FAR	VR@0.1FAR
3	98.81%%	0.07%	100.00%	97.62%
4	98.81%	0.09%	100.00%	97.62%
5	98.81%	0.09%	100.00%	97.62%
6	98.81%	0.04%	100.00%	98.81%
7	100.00%	0.00%	100.00%	100.00%
8	100.00%	0.00%	100.00%	100.00%
9	100.00%	0.00%	100.00%	100.00%
10	100.00%	0.00%	100.00%	100.00%

According to the results in Table 19, which indicate that the accuracy of recognition tests improves with an increase in the number of orientations, we found that using a Gabor filter bank with 9 scales, an orientation factor of 7 or above, and a fixed down sampling factor of 64 bits for the left-hand vein 950 resulted in the highest Rank-1 recognition rate of 100.00%, with an absence of Equal Error Rate (EER). Additionally, VR@1% FAR and VR@0.1% FAR values indicate that the system can verify 100.00% of both samples with high accuracy, demonstrating the effectiveness of the Gabor filter bank. This means that all users were correctly identified without errors.

- The following **Figure III. 11** presents an example of the Gabor filter bank applied to an image of the left-hand vein 950 with different parameter:

Original image

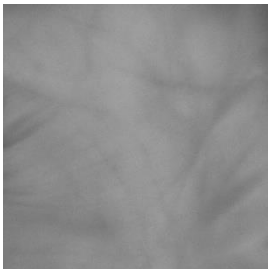

Orientation	Wavelength	Magnitude	Phase
0	4	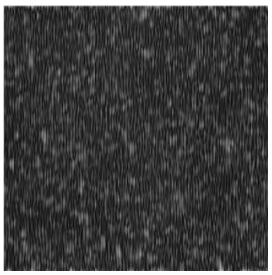	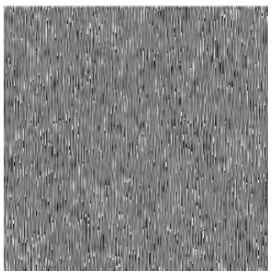
0	8	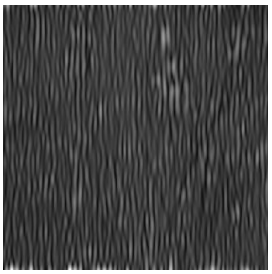	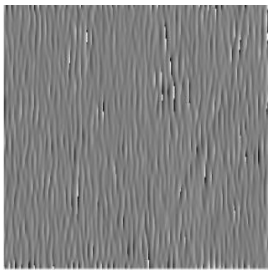
90	4	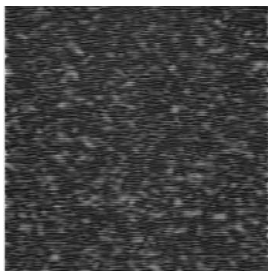	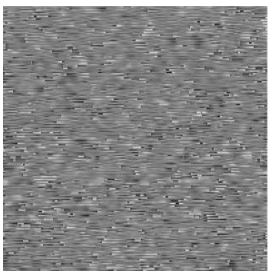
90	8	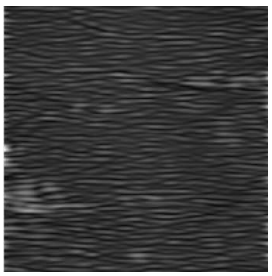	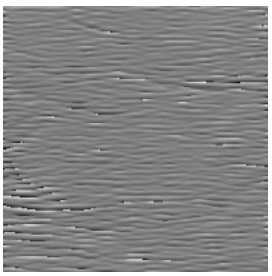

Figure III. 11: Example of the Gabor filter bank applied to an image of the left-hand vein 950

III.3.2.5Results of our method utilizing the left-hand vein 850

Table 20: represents the Identification and Verification mode for Gabor filter bank scales (with a fixed orientation value) using the left-hand vein 850. It shows that increasing the number of scales significantly improves the system's performance in terms of recognition rate, error rate, VR@1% FAR, and VR@0.1% FAR. The best results were achieved when fixing the number of orientations at 2 and setting the down sampling factor to 64 bits. In this case, a Rank-1 recognition rate of 95.24% was achieved for identity recognition, with an Equal Error Rate (EER) of 2.38%. Additionally, VR@1% FAR and VR@0.1% FAR values indicate that the system can verify 95.24% of both samples with high accuracy at scale 10.

Table 20: Rank -1/EER results of Gabor filter bank scales for left hand vein 850

Num_of_scales	Identification	Verification		
	Rank (%)	EER (%)	VR@1FAR	VR@0.1FAR
2	27.38%	21.81%	25.00%	9.52%
3	40.48%	20.09%	35.71%	14.29%
4	60.71%	16.61%	61.90%	28.57%
5	73.81%	8.33%	76.19%	58.33%
6	88.10%	4.59%	89.29%	79.76%
7	91.67%	2.38%	96.43%	88.10%
8	94.05%	2.38%	97.62%	89.29%
9	94.05%	2.38%	96.43%	91.67%
10	95.24%	2.38%	95.24%	95.24%
11	95.24%	2.38%	95.24%	95.24%

Table 21: represents the identification and verification mode for Gabor filter bank scales (with a fixed scale value) for the left-hand vein 850 based on the results found in Table 20. We fixed the Gabor filter bank at scale 10 and the down sampling factor at 64 bits. In this case, we varied the orientation value, resulting in the following outcomes

Table 21: Rank -1/EER results of Gabor filter bank orientation for left hand vein 850

Num_of_orient	Identification	Verification		
	Rank (%)	EER (%)	VR@1FAR	VR@0.1FAR
3	96.43%	1.19%	98.81%	96.43%
4	96.43%	1.48%	97.62%	96.43%
5	96.43%	1.41%	97.62%	96.43%
6	96.43%	1.07%	100.00%	96.43%
7	98.81%	0.10%	100.00%	97.62%
8	98.81%	0.09%	100.00%	98.81%
9	98.81%	0.09%	100.00%	98.81%
10	98.81%	0.09%	100.00%	98.81%

According to the results in Table 21, which indicate that the accuracy of recognition tests improves with an increase in the number of orientations, we found that using a Gabor filter bank with 10 scales, an orientation factor of 8 or above, and a fixed down sampling factor of 64 bits for the left-hand vein 850 resulted in the highest Rank-1 recognition rate of 98.81%, with an Equal Error Rate (EER) of 0.09% for verification. Additionally, VR@1% FAR and VR@0.1% FAR values indicate that the system can verify 100.00% and 98.81% of the samples respectively compared to other scale parameter values.

- The following **Figure III. 12** presents an example of the Gabor filter bank applied to an image of the left-hand vein 850 with different parameter:

Original image

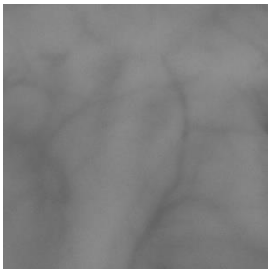

Orientation	Wavelength	Magnitude	Phase
0	4	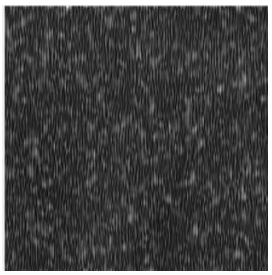	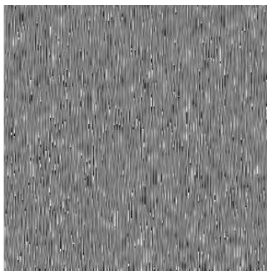
0	8	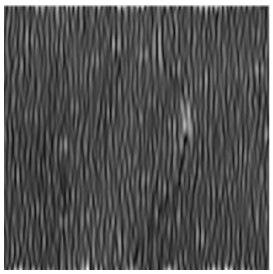	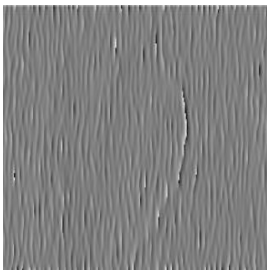
90	4	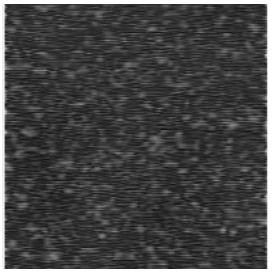	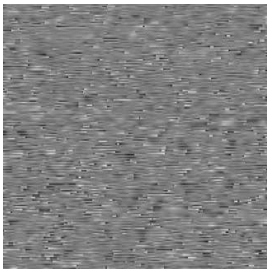
90	8	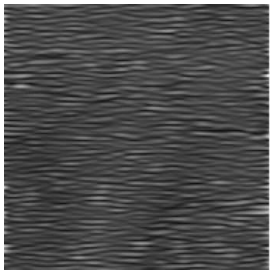	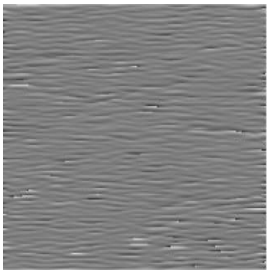

Figure III. 12: Example of the Gabor filter bank applied to an image of the left-hand vein 850

III.4 Multimodal biometric system for score-level fusion:

The known multimodal biometric system involves the integration of two or more biometric traits for authentication, as it is difficult to spoof multiple biometric sources simultaneously. The following tables present the multimodal biometric system for feature-level fusion of two different traits using LPQ and GABOR filter bank.

Table 22: represents Identification and Verification mode for the combined features of the left index finger and left-hand vein 850 using GABOR filter bank, where we selected the best result for the two features. In the left index finger feature, at scale 13 and orientation 7, and in the second feature left hand vein 850 at scale 10 and orientation 8. The experimental results for combining the features showed that multimodal biometric systems outperform unimodal systems.

The results obtained in the table below show that the configurations of Simple-sum fusion, Min-score fusion, and Matcher weighting fusion yielded similar results, achieving a Rank-1 recognition rate of 98.81%. Additionally, there was a very low Equal Error Rate (EER) of 0.09% for verification. Furthermore, the values of the verification rate at 1% FAR equals (%) and the verification rate at 0.1% FAR equals (%) were both 98.81%, indicating the effectiveness of the multimodal biometric fusion system for diverse features.

Table 22: Rank -1/EER results of Gabor filter bank for the combined features of the left index finger and left-hand vein

score-level fusion	Identification	Verification		
	Rank-1 %	EER %	VR@1FAR	VR@0.1FAR
Simple-sum fusion	98.81%	0.09%	100.00%	98.81%
Min-score fusion	98.81%	0.09%	100.00%	98.81%
Max-score fusion	96.43%	3.56%	96.43%%	94.05%
Matcher weighting fusion	98.81%	0.09%	100.00%	98.81%

Table 23: represents the identification and verification modes for the combined features of the left index finger and left-hand vein 950 using the LPQ method, showcasing the best results for both features. For the left index finger, the optimal parameters were a window size of 21 and a block size of 225, while for the left-hand vein 950, the optimal parameters were a window size of 25 and a block size of 25. The experimental results demonstrated that multimodal biometric systems outperform unimodal systems.

The results in the table below show that the Simple Sum Fusion, Minimum Score Fusion, and Matcher Weight Fusion configurations yielded similar results, achieving a first-rank recognition rate of 100.00%. In addition, the EER was very low at 0.00% for verification. Moreover, the verification rate at 1% FAR and the verification rate at 0.1% FAR were both 100.00%. In contrast, the Max Score Fusion had a lower first-rank recognition rate of 96.43% and an EER of 3.38%, indicating the effectiveness of the multimodal biometric fusion system for various features.

Table 23 : Rank -1/EER results of LPQ method for the combined features of the left index finger and left-hand vein

Score -level fusion	Identification	Verification		
	Rank-1 %	EER %	VR@1FAR	VR@0.1FAR
Simple- sum fusion	100.00%	0.00%	100.00%	100.00%
Min-score fusion	100.00%	0.00%	100.00%	100.00%
Max-score fusion	96.43%	3.38%	96.43%	96.43%
Matcher weighting fusion	100.00%	0.00%	100.00%	100.00%

III.5 CMC curve:

The Cumulative Match Characteristic (CMC) curve is a widely used performance evaluation metric for biometric systems, especially in identification mode. The two figures below show examples of CMC curves from our experiments using LPQ and Gabor filters (see **Figure III. 13**).

(a) (b)

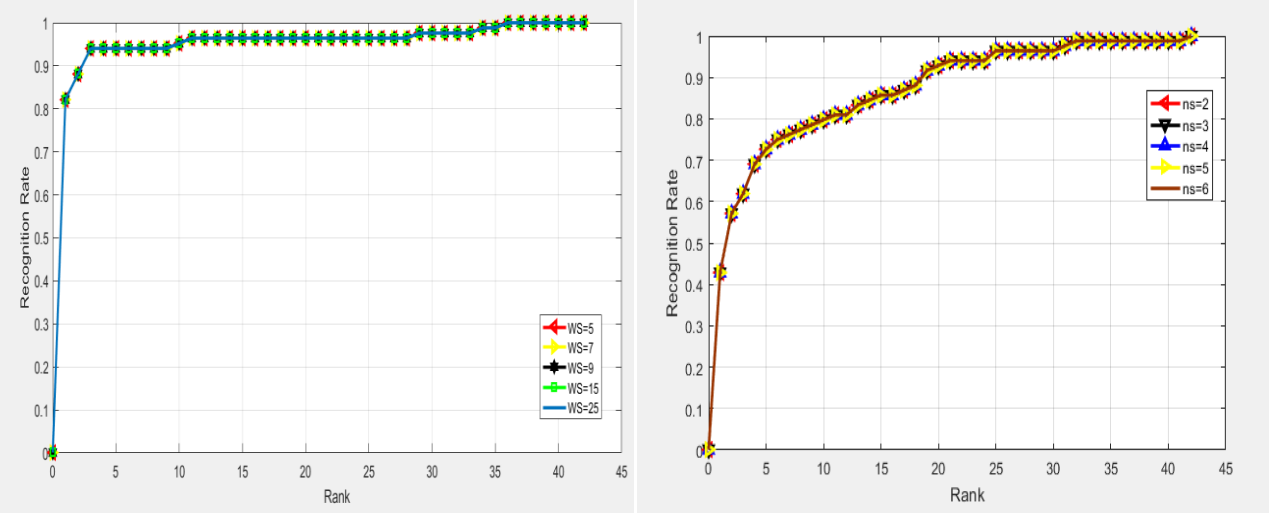

Figure III. 13: (a) Example of a CMC curve using the LPQ method, (b) Example of a CMC curve using the Gabor filter bank

III.6 Comparative Analysis:

A comparative analysis of vein-based authentication is provided in Table 1. All the results presented in this table are expressed in terms of Equal Error Rate (EER). The Equal Error Rate (EER) is defined as the point where FAR equals FRR. Lower EER values indicate better system performance, but these values can vary depending on the imaging technique, type of biometric trait, methodologies used for feature extraction, method and type of fusion of these features, and the number of users in the database.

Table 24: Comparative Analysis between Our Work and Related Work

Reference	Biometric features	Methodology	Imaging	Database	Performance
Ferrer,M.A., Morales,A., Travieso,C.M .andAlonso, J.B [40]	Hand geometry, palm and finger textures, dorsal hand vein	Simple Sum rule	Near IR imaging	50 users	EER = 0.01
Yuksel, A., and Akarun, L [41]	Hand vein	ICA 1, ICA2, LEM and NMF	Near IR imaging	100 users	EER=5.4, 7.24,7.64 and 9.17
Contactless[71]	Finger vein	MC / PC / GF and SIFT	Near IR imaging	42 users /840images	EER=3.66%
	Hand vein	MC / PC / GF and SIFT	Near IR imaging	42users /420images	EER=0.35%
Our Works	Palm vein	LPQ method	Near IR imaging	42 users /840images	EER =0.00
		Gabor filter bank	Near IR imaging	42 users /840images	EER =0.00
	finger vein	LPQ method	Near IR imaging	42 users /210images	EER =3.56
		Gabor filter bank	Near IR imaging	42 users /210images	EER =5.95

Conclusion

In the final chapter, we delved into the experimental study of our work, where we developed a system for person identification based on hand vein and finger vein using the methods and algorithms outlined in the previous chapter. Features of each biometric trait were captured, extracted, presented, and classified. We utilized a database consisting of 42 individuals and 1050 images. To achieve optimal results, we introduced several biometric systems (hand vein/left index finger), including both unimodal and multimodal systems (relying on the fusion and recognition of both finger vein and hand vein together).

The system's effectiveness was evaluated using Rank-1 identification rate, Equal Error Rate (EER), and verification rates at 1% and 0.1% FAR. The system achieved a 100% identification rate and 0% error rate, demonstrating the quality of our vein recognition and affirming its potential for biometric applications.

General Conclusion and future work:

The popularity of vein-based biometric systems is increasing due to their possession of the four biometric characteristics (universality, uniqueness, permanence, and resistance to circumvention). The work carried out in this dissertation aims to study this system, where we designed a practical and intelligent biometric recognition system based on identifying the palm vein of the left hand's index finger and integrating it. Our system includes the following two steps: Region of Interest (ROI) determination, vein pattern feature extraction, and recognition. We used a database that does not require preprocessing as it was captured by near-infrared radiation.

In this system, we utilized LPQ and GABOR methods for feature extraction, and we worked on individual recognition algorithms using K-NN classification methods. Thanks to these methods, we achieved perfect accuracy after applying this system to a database comprising 42 individuals and 1050 images. The achieved results were quite remarkable as we obtained a Rank-1 recognition and identification rate of 100%, an Equal Error Rate (EER) of 0.00%, and verification rates (VR) of 100% at error rates of 1% and 0.1%. These results demonstrate the potential and feasibility of using hand veins and fingers as a biometric means for multi-purpose identification. Additionally, these results make our system reliable and achieve the goal we set initially, which is to identify users for both single-mode and multi-mode systems completely and without errors.

In future work, we aim to use a larger database containing more users. In addition to using feature extraction techniques and other pre-processing methods to test them with our system. Furthermore, we will install a vein capture device for the finger and palm veins.

References:

[1] KAK, Neha; GUPTA, Rishi; MAHAJAN, Sanchit. Iris recognition system. International Journal of Advanced Computer Science and Applications, 2010, 1.1.

[2] ALI, A. Tahseen; ABDULLAH, Hasanen S.; FADHIL, Mohammad N. Voice recognition system using machine learning techniques. Materials Today: Proceedings, 2021, 1-7.

[3] ALI, Mouad MH, et al. Overview of fingerprint recognition system. In: 2016 international conference on electrical, electronics, and optimization techniques (ICEEOT). IEEE, 2016. p. 1334-1338.

[4] KORTLI, Yassin, et al. Face recognition systems: A survey. Sensors, 2020, 20.2: 342.

[5] MARATTUKALAM, Felix, et al. Deep Learning-Based Wrist Vascular Biometric Recognition. Sensors, 2023, 23.6: 3132.

[6] YUKSEL, Aycan; AKARUN, Lale; SANKUR, Bulent. Hand vein biometry based on geometry and appearance methods. IET computer vision, 2011, 5.6: 398-406.

[7] SOUAD, KHELLAT KIHEL. Identification biométrique par fusion multimodale de l'empreinte d'articulation, l'empreinte digitale et l'empreinte veineuse du doigt. 2017. PhD Thesis. Université Mohamed Boudiaf des sciences et de la technologi.

[8] BOUCETTA, Aldjia. Approches évolutionnaires multi-biométriques pour l'identification des personnes. 2019. PhD Thesis. Université de Batna 2.

[9] TIN, K. H. H. An effective method of a person's character or future using the palmprint images. International Journal of Research and Scientific Innovation, 2016, 4.

[10] MOULAY, M.; ARBAOUI, M. authentification des personnes parl'articulation du doigt. UNIVERSITE KASDI MERBAHOUARGLA, 2015.

[11] BAHMED, Farah; OULD MAMMAR, Madani. Basic finger inner-knuckle print: A new hand biometric modality. IET Biometrics, 2021, 10.1: 65-73

[12]BOURENEB, AZIZA. Identification des personnes par leursempreintes palmaire. 2019.

[13] 5. Yanagawa, T., Aoki, S., Ohyama, T.: Human finger vein images are diverse and its patterns are useful for personal identification. MHF Preprint Series, pp. 1–7 (2007)

[14] Heenaye-mamode Khan, M., Subramanian, R.K., Mamode Khan, N.A.: Low dimensional representation of dorsal hand vein features using Principle Component Analysis. In: The Proceedings of World Academy of Science, Engineering and Technology, pp. 1091–1097 (2009)

[15] Ladoux, P.-O., Rosenberger, C., Dorizzi, B.: Palm vein verification system based on SIFT matching. In: Tistarelli, M., Nixon, M.S. (eds.) ICB 2009. LNCS, vol. 5558, pp. 1290– 1298. Springer, Heidelberg (2009).

[16] JIN, Ling. Using deep learning for finger-vein based biometric authentication.URL: https://towardsdatascience.com/using-deep-learning-for-finger-vein-based-biometric-authentication-3f6601635821 (accessed March 23, 2023).

[17] "Extraction of Finger-Vein Patterns Using Maximum Curvature Points in Image Profiles," in Proceedings of the 9th IAPR Conf. on Machine

Vision Applications, N. Miura, A. Nagasaka, and T. Miyatake, (MVA2005, Tsukuba Science City, Japan, 2005), pp. 347-350.

[18] Bio-informatics Visualization Technology committee, Bio-informatics Visualization Technology (Corona Publishing, 1997), p.83, Fig.3.2.

[19] CHAA, Mourad. Person recognition system using biometric techniques. 2017. PhD These. .Ferhat Abbas University

[20] HEZIL,Nabil; BOUKROUCHE, Abdelhani. Multimodal biometricrecognition using human ear and palmprint. IET Biometrics2017, 6.5: 351-359

[21]DALE, Manisha P.; JOSHI, Madhuri A.; GILDA, Neena. Texture based palmprint identification using DCT features. In: 2009 Seventh International Conference on Advances in Pattern Recognition. IEEE, 2009. p. 221-224.

[22] EL-ABED, Mohamad; CHARRIER, Christophe. Evaluation of biometric systems. New Trends and Developments in Biometrics, 2012, pp. 149-169.

[23] ROSS, Arun. Relating ROC and CMC curves. 2016.

[24] MALIK, Jyoti, et al. Reference threshold calculation for biometric authentication. IJ Image, Graphics and Signal Processing, 2014, 2: 46-53.

[25] DU, Yingzi; CHANG, Chein-I. Rethinking the effective assessment of biometric systems. SPIE Newsroom, 2007, 1-3.

[26] ABABSA, Souhila Guerfi. Authentification d'individus par reconnaissance de caractéristiques biométriques liées aux visages 2D/3D. Evry-Val d'Essonne, 2008.

[27] RAHIM, Md Saifur. An optimal score fusion strategy for a multimodal biometric authentication system for mobile device. 2010.

[28] ALSAADE, Fawaz; ZAHRANI, Mohammed; ALGHAMDI, Turki. Score-Level Fusion in Biometric Verification. In: 2013 International Symposium on Biometrics and Security Technologies. IEEE, 2013. p. 193-197.

[29] CHIA, Chaw; SHERKAT, Nasser; NOLLE, Lars. Towards a best linear combination for multimodal biometric fusion. In: 2010 20th international conference on pattern recognition. IEEE, 2010. p. 1176-1179.

[30] Guennouni S, Mansouri A, Ahaitouf A. Biometric systems and their applications. Visual impairment and blindness-what we know and what we have to know. 2020 Sep 9.

[31] KHERROUBI, MIMOUNA; TIDJANI, HALA. Reconnaissance des personnes par finger Vein. PhD Thesis. UNIVERSITE KASDI MERBAH OUARGLA.

[32] LOVATO, Juniper L. Group-Level Frameworks for Data Ethics, Privacy, Safety and Security in Digital Environments. The University of Vermont and State Agricultural College, 2023.

[33] YUKSEL, Aycan; AKARUN, Lale; SANKUR, Bulent. Hand vein biometry based on geometry and appearance methods. IET computer vision, 2011, 5.6: 398-406.

[34] LHUAIRE, Martin, et al. Venous system mapping of the digits and the hand: An anatomical study and potential surgical applications. JPRAS open, 2022, 33: 171-183.

[35] ZHAO, Yuan; SHENG, Ming-Yu. Acquisition and preprocessing of hand vein image. In: 2011 International Conference on Multimedia Technology. IEEE, 2011. p. 5727-5729.

[36] BOSSARD, Antoine. Memory Optimisation on AVR Microcontrollers for IoT Devices' Minimalistic Displays. Chips, 2022, 1.1: 2-13.

[37] VAN ROON, Gideon. Board design and implementation for 8-bit avr microcontrollers in an educational environment. 2018.

[38] KUMAR, Ajay; PRATHYUSHA, K. Venkata. Personal authentication using hand vein triangulation and knuckle shape. IEEE Transactions on Image processing, 2009, 18.9: 2127-2136.

[39] RAGHAVENDRA, Ramachandra, et al. Multimodal biometrics: Analysis of handvein & palmprint combination used for person verification. In: 2010 3rd International Conference on Emerging Trends in Engineering and Technology. IEEE, 2010. p. 526-530.

[40] FERRER, Miguel A., et al. Combining hand biometric traits for personal identification. In: 43rd Annual 2009 International Carnahan Conference on Security Technology. IEEE, 2009. p. 155-159.

[41] YÜKSEL, Aycan; AKARUN, Lale; SANKUR, Bulent. Biometric identification through hand vein patterns. In: 2010 International Workshop on Emerging Techniques and Challenges for Hand-Based Biometrics. IEEE, 2010. p. 1-6.

[42] WANG, Yiding, et al. Hand vein recognition based on multiple keypoints sets. In: 2012 5th IAPR International Conference on Biometrics (ICB). IEEE, 2012. p. 367-371.

[43] AHMED, Mona A.; ROUSHDY, Mohamed; SALEM, Abdel-Badeeh M. Intelligent technique for human authentication using hand vein. International Journal of Data Science, 2020, 5.4: 263-275.

[44] CROSS, J. M.; SMITH, C. L. Thermographic imaging of the subcutaneous vascular network of the back of the hand for biometric identification. In: Proceedings The Institute of Electrical and Electronics Engineers. 29th Annual 1995 International Carnahan Conference on Security Technology. IEEE, 1995. p. 20-35.

[45] TANAKA, Toshiyuki; KUBO, Naohiko. Biometric authentication by hand vein patterns. In: SICE 2004 Annual Conference. IEEE, 2004. p. 249-253.

[46] LIN, Chih-Lung; FAN, Kuo-Chin. Biometric verification using thermal images of palm-dorsa vein patterns. IEEE Transactions on Circuits and systems for Video Technology, 2004, 14.2: 199-213.

[47] WANG, Lingyu; LEEDHAM, Graham. A thermal hand vein pattern verification system. In: International Conference on Pattern Recognition and Image Analysis. Berlin, Heidelberg: Springer Berlin Heidelberg, 2005. p. 58-65.

[48] DING, Yuhang; ZHUANG, Dayan; WANG, Kejun. A study of hand vein recognition method. In: IEEE International Conference Mechatronics and Automation, 2005. IEEE, 2005. p. 2106-2110.

[49] WANG, Kejun, et al. Hand vein recognition based on multi supplemental features of multi-classifier fusion decision. In: 2006 international conference on mechatronics and automation. IEEE, 2006. p. 1790-1795.

[50] WANG, Zhongli, et al. A performance evaluation of shape and texture based methods for vein recognition. In: 2008 Congress on Image and Signal Processing. IEEE, 2008. p. 659-661.

[51] YUKSEL, Aycan; AKARUN, Lale; SANKUR, Bulent. Hand vein biometry based on geometry and appearance methods. IET computer vision, 2011, 5.6: 398-406.

[52] HSU, Chih-Bin, et al. Combining local and global features based on the eigenspace for vein recognition. In: 2012 International Symposium on Intelligent Signal Processing and Communications Systems. IEEE, 2012. p. 401-405.

[53] DAS, Ravi. Biometric technology: authentication, bio cryptography, and cloud-based architecture. CRC press, 2014.

[54] HEIKKILA, Janne; OJANSIVU, Ville. Methods for local phase quantization in blur-insensitive image analysis. In: 2009 International Workshop on Local and Non-Local Approximation in Image Processing. IEEE, 2009. p. 104-111.

[55] SUPREETHA GOWDA, H. D.; HEMANTHA KUMAR, G.; IMRAN, Mohammad. Multi-modal biometric system on various levels of fusion using LPQ features. Journal of Information and Optimization Sciences, 2018, 39.1: 169-181.

[56] BARBU, Tudor. Gabor filter-based face recognition technique. Proceedings of the Romanian Academy, 2010, 11.3: 277-283.

[57] CHAA, Mourad, et al. An efficient biometric based personal authentication system using Finger Knuckle Prints features. In: 2016 International Conference on Information Technology for Organizations Development (IT4OD). IEEE, 2016. p. 1-5..

[58] STEINBACH, Michael; TAN, Pang-Ning. kNN: k-nearestneighbors. In: The top ten algorithms in data mining. Chapmanand Hall/CRC, 2009. p. 165-176.

[59] Vimal, A., Valluri, S.R., Karlapalem, K.: An experiment with distance measures for clustering. Technical report, Center of Data Engineering, IIIT, Hyderabad (2008)

[60] Duda, R.O., Hart, P.E., Stork, D.G.: Pattern Recognition. John Wiley and Sons (2001)

[61] Xu, R., Wunsch, D.: Survey of clustering algorithms. IEEE Trans. Neural Networks. 16(3), 513–521 (2005)

[62]Jain, A.K., Dubes, R.C.: Algorithms for clustering data. Prentice Hall, Englewood Cliffs, NJ (1988).

[63] Mahalanbois, P.C.: On the generalized distance in statistics. In: Naitional Institute of Sciences of India, pp.49–55. Chicago (1936)

[64] ABBAD, ABDELGHAFOUR; TAIRI, HAMID. Combining Jaccard and Mahalanobis Cosine distance to enhance the face recognition rate. WSEAS Transactions on Signal Processing, 2016, 16: 171-178.

[65]OKOYE, Kingsley, et al. Machine learning model (RG-DMML)and ensemble algorithm for prediction of students' retention andgraduation in education. Computers and Education: ArtificialIntelligence, 2024, 6: 100205.

[66]HASAN, Quazi Mainul. Typifying Wikipedia Articles. TheUniversity of Texas at Arlington, 2010

[67] BERWICK, Robert. An Idiot's guide to Support vector machines (SVMs). Retrieved on October, 2003, 21: 2011.

[68] http://www.wavelab.at/sources/PLUSVein-Contactless/ LAST 10 / 05 /2024

[69] . Lu, Y.; Xie, S.J.; Yoon, S.; Wang, Z.; Park, D.S. An available database for the research of finger vein recognition. In Proceedings of the 2013 6th International Congress on Image and Signal Processing (CISP), Hangzhou, China, 16–18 December 2013; Volume 1, pp. 410–415

[70] Zhou, Y.; Kumar, A. Human identification using palm-vein images. IEEE Trans. Inf. Forensics Secur. 2011, 6, 1259–1274. [CrossRef]

[71] KAUBA, Christof; PROMMEGGER, Bernhard; UHL, Andreas. Combined fully contactless finger and hand vein capturing device with a corresponding dataset. Sensors, 2019, 19.22: 5014.